

**STRUCTURE RHEOLOGY OF
CARBOXYMETHYL CELLULOSE (CMC)
SOLUTIONS**

A Thesis

**Submitted to the College of Engineering of
Nahrain University in Partial Fulfillment of the
Requirements for the Degree of Master of Science in
Chemical Engineering.**

**by
Mustafa Jaafar Nayef
B.Sc. in Chemical Engineering 2006**

**Safar
February**

**1432
2011**

CERTIFICATION

I certify that this thesis entitled “**STRUCTURE RHEOLOGY OF CARBOXYMETHYL CELLULOSE (CMC) SOLUTIONS**” was prepared by **Mustafa Jaafar Nayef** under my supervision at Nahrain University, College of Engineering, in partial fulfillment of the requirements for the degree of Master of Science in Chemical Engineering.

Signature: 
Name: Prof. Dr. Talib Kashmoula
(Supervisor)
Date: 24 / 02 / 2011

Signature: 
Name: Asst. Prof. Dr. Basim O. Hassan
(Head of Department)
Date: 28 / 2 / 2011

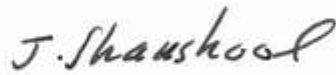
CERTIFICATE

We certify, as an examining committee, that we have read this thesis entitled "STRUCTURE RHEOLOGY OF CARBOXYMETHYL CELLULOSE (CMC) SOLUTIONS" examined the student **Mustafa Jaafar Nayef** in its content and found it meets the standard of thesis for the degree of Master of Science in Chemical Engineering.

Signature: 
Name: Prof. Dr. Talib Kashmoula
(Supervisor)
Date: 24 / 02 / 2011

Signature: 
Name: Asst. Prof. Dr. Khalid A. Sukkar
(Member)
Date: 24 / 2 / 2011

Signature: 
Name: Dr. G. A. Mohammed
(Member)
Date: 24 / 2 / 2011

Signature: 
Name: Prof. Dr. Jabir Shanshool
(Chairman)
Date: 24 / 2 / 2011

Approval of the College of Engineering

Signature: 
Name: Prof. Dr. Muhsin J. Jweeg
(Dean)
Date: 28 / 2 / 2011

ABSTRACT

Rheological study on carboxymethyl cellulose (CMC) dissolved in (6% NaOH in Water) solution was undertaken; Seven grades of carboxymethyl cellulose had been used.

The Mw data were obtained by M-H equation using intrinsic viscosity data, which are obtained based on viscosity measurement. (19,918, 45,700, 76,693, 83,139, 148,800) gm/cm³.

The values of Huggins coefficient (K_H) have been obtained from plotting (η_{red} vs conc.). (1.135, 0.3, 3.448, 0.473, 0.059)gm/mol.

The flow curves have been measured for different molecular weights with different concentrations, which lead to estimation the viscosity (η_o) at shear rate zero.

The concentrated region involved the determination of the network parameters (M_e , $A(C)$) by plotting η_o versus Mwt in log-log scale it may lead to determine the critical molecular weight (M_c) the transition point from particle to network region,.

List of Contents

	<u>Page</u>
Abstract	I
List of Contents	II
Nomenclature	IV
List of Tables	VI
List of Figures	VIII
CHAPTEER ONE: INTRODUCTION	1
CHAPTER TWO : LITERATURE SURVEY	5
2.1 Polysaccharide	5
2.1.1 Commercial Applications	7
2.2 Rheology	13
2.3 Types Of Polymer Solution	13
2.3.1 The Particle Solution (Dilute-Solution)	14
2.3.2 The Network Solution (Semidilute and Concentrated-Solution)	24
2.4 Review of Local Work In Al-Nahrain Univesity	29
CHAPTER THREE :EXPERIMENTAL WORK	
3.1 Materials	33
3.2 Preparation of solution	33
3.3 Apparatus	34
3.4 Measurement of viscosity	34
3.4.1 Dilute solution	34
3.4.2 Concentrated solution	37

CHAPTER FOUR : RESULTS AND DISCUSSION

4-1	Intrinsic Viscosity Calculation	39
4-2	Measurement of dynamic viscometer with rotational viscometer for Concentrated solution calculation	47

CHAPTER FIVE : CONCLUSIONS AND RECOMMENDATIONS

5.1	Conclusions	77
5.2	Recommendations for Future Work	77

REFERENCES	78
-------------------	----

APPENDICES

Appendix A	A-1
Appendix B	B-1
Appendix C	C-1

Nomenclature

Symbols

Notations

English Alphabet

A' (C)	Apparent Statistical chain element	$\overset{\circ}{\text{A}}$
a	Exponent in the Mark–Houwink–Sakurada equation	----
A	Statistical chain element	$\overset{\circ}{\text{A}}$
C	Solute concentration	gm/cm ³
f_o	Fractional free volume at T _g	-----
$\sqrt{\overline{h^{-2}}}$	Mean square end-to-end distance of coil	cm
K	Constant in the Mark–Houwink–Sakurada equation	-----
k'	Huggins's constant	-----
k''	Kraemer's constant	-----
L	Length of polymer chain	cm
L_o	monomer length	cm
M	Molecular weight	gm/mol
M_n	number-average molecular weight	gm/mol
m_o	monomer length	
M_v	Viscosity-average molecular weight	gm/mol
M_w	Weight-average molecular weight	gm/mol
n_2	Number of molecules	gm/mol

N_L	Avogadro's number	molecule mol ⁻¹
R_e	Hydrodynamic sphere equivalent radius	cm
R_{eo}^2/M	Roughly constant	-----
\bar{r}_0^2	Mean square end-to-end distance of the unperturbed coil	cm ²
T_g	Glass transition temperature	C°
V	Volume fraction	-----
v_2	Volume fraction of polymer	-----
V_e	Hydrodynamic sphere volume	cm ³

Greek Alphabet

α	Expansion of a polymer coil in a good solvent	-----
η	Viscosity of a solution	cp
$[\eta]$	Intrinsic viscosity	cm ³ /gm
η_o	Zero RPM apparent viscosity	cp
η_{rel}	Relative viscosity	-----
η_{red}	Reduction viscosity	cm ³ /gm
η_s	Viscosity of the solvent	cm ³ /gm
η_{sp}	Specific viscosity	cm ³ /gm
π	Osmotic pressure	bar
π_1	3.1416	-----
Φ	Universal constant in intrinsic viscosity	-----

List of Tables

<u>Table</u>	<u>Title</u>	<u>Page</u>
2.1	Main Practical Uses of Xanthan for the Food Industry	8
2.2	$[\eta]$ and Mwt for Novolak in Acetone	30
2.3	$[\eta]$ and Mwt for Polyvinyl alcohol in water	30
2.4	$[\eta]$ and Mwt for Polyethylen glycol in water	31
2.5	$[\eta]$ and Mwt for polychloroprene in toluene	31
4.1	Results of Huggins coefficient and intrinsic viscosity for five grades of Carboxymethyl cellulose	45
4-2	Results of intrinsic viscosity and molecular weight for five grades of Carboxymethyl cellulose.	46
4-3	the results of power law calculation for concentration 1%	68
4-4	the results of power law calculation for concentration 2%	68
4-5	the results of power law calculation for concentration 3%	69
4-6	the results of power law calculation for concentration 4%	69
4-7	Π_o and Mv of each CMC sample with all Conc.	70
4-8	Me and A(c) of CMC for all conc	75
A-1	Values of the Mark–Houwink–Sakurada exponent a	A-1
B-1	Time, Π_{sp} and Π_{red} for CMC1.	B-1
B-2	Time, Π_{sp} and Π_{red} for CMC2.	B-1
B-3	Time, Π_{sp} and Π_{red} for CMC3.	B-1
B-4	Time, Π_{sp} and Π_{red} for CMC4.	B-2
B-5	Time, Π_{sp} and Π_{red} for CMC5.	B-2

C-1	η and RPM of each CMC sample with conc. 1%.	C-1
C-2	η and RPM of each CMC sample with conc. 2%.	C-2
C-3	η and RPM of each CMC sample with conc. 3%.	C-3
C-4	η and RPM of each CMC sample with conc. 4%.	C-4

List of Figures

<u>Figure</u>	<u>Title</u>	<u>Page</u>
1-1	Chemical structure of CMC.	4
2-1	chemical structure of xanthan repeating unit.	5
2-2	The effect of shear rates on polymer chain rotation	15
2-3	The equivalent sphere model	18
2-4	Schematic of a plot of η_{sp}/c and $\ln\eta_{rel}/c$ versus c , and extrapolation to zero concentration to determine $[\eta]$.	22
2-5	Double logarithmic plots of $[\eta]$ versus M_w for anionically synthesized polystyrenes, which were then fractionated leading to values of M_w/M_n of less than 1.06. Filled circles in benzene, half-filled circles in toluene, and open circles in dichloroethylene, all at 30°C. The arrows indicate the axes to be used.	24
2-6	Relationship between apparent viscosity and (a) concentration at constant molecular weight; (b) molecular weight at constant concentration	25
2-7	Relationships of polymer chains in solution at different concentration regions. (a) Dilute solution regime (b) The transition regions,(c) Semi-dilute regime.	26
2-8	The chain element concept.	27
3-1	BS/U-Tube Viscometer type D.	37
3-2	Rotational viscometer.	38
4-1	Relationship between concentration and reduction viscosity for	40

<u>Figure</u>	<u>Title</u>	<u>Page</u>
	CMC1.	
4-2	Relationship between concentration and reduction viscosity for	41
	CMC2.	
4-3	Relationship between concentration and reduction viscosity for	42
	CMC3.	
4-4	Relationship between concentration and reduction viscosity for	43
	CMC4.	
4-5	Relationship between concentration and reduction viscosity for	44
	CMC5.	
4-6	Relationship between η and RPM for CMC1 for Conc. 1%.	48
4-7	Relationship between η and RPM for CMC2 for Conc. 1%.	49
4-8	Relationship between η and RPM for CMC3 for Conc. 1%.	50
4-9	Relationship between η and RPM for CMC4 for Conc. 1%.	51
4-10	Relationship between η and RPM for CMC5 for Conc. 1%.	52
4-11	Relationship between η and RPM for CMC1 for Conc. 2%.	53
4-12	Relationship between η and RPM for CMC2 for Conc. 2%.	54
4-13	Relationship between η and RPM for CMC3 for Conc. 2%.	55
4-14	Relationship between η and RPM for CMC4 for Conc. 2%.	56
4-15	Relationship between η and RPM for CMC5 for Conc. 2%.	57
4-16	Relationship between η and RPM for CMC1 for Conc. 3%.	58
4-17	Relationship between η and RPM for CMC2 for Conc. 3%.	59
4-18	Relationship between η and RPM for CMC3 for Conc. 3%.	60
4-19	Relationship between η and RPM for CMC4 for Conc. 3%.	61
4-20	Relationship between η and RPM for CMC5 for Conc. 3%.	62

<u>Figure</u>	<u>Title</u>	<u>Page</u>
4-21	Relationship between η and RPM for CMC1 for Conc. 4%.	63
4-22	Relationship between η and RPM for CMC2 for Conc. 4%.	64
4-23	Relationship between η and RPM for CMC3 for Conc. 4%.	65
4-24	Relationship between η and RPM for CMC4 for Conc. 4%.	66
4-25	Relationship between η and RPM for CMC5 for Conc. 4%.	67
4-26	Relationship between $\log \Pi_0$ and $\log Mwt$ for Conc. 1%.	71
4-27	Relationship between $\log \Pi_0$ and $\log Mwt$ for Conc. 2%.	72
4-28	Relationship between $\log \Pi_0$ and $\log Mwt$ for Conc. 3%.	73
4-29	Relationship between $\log \Pi_0$ and $\log Mwt$ for Conc. 4%.	74
4-30	Relationship between $A(c)$ and Conc	75
4-31	Relationship between η and time at fixed RPM (100) for CMC (1,4,7)	76

CHAPTER ONE

INTRODUCTION

Rheology describes the deformation and flow of body under the influence of stresses (Bodies) in this context can be either solids, liquids, or gases[Gebhard, 2000].It applies to substances which have a complex structure, including muds, sludges, suspensions, polymers, many foods, bodily fluids, and other biological materials. The flow of these substances cannot be characterized by a single value of viscosity (at a fixed temperature) -instead the viscosity changes due to other factors.

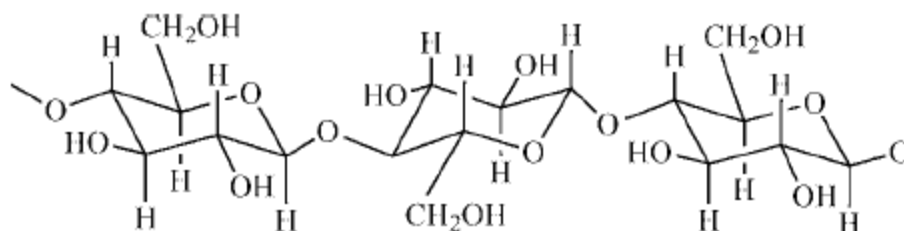
Intrinsic viscosity is the limiting value of the reduced viscosity as the concentration approaches zero [Barnes et. al., 1989]. Many foods contain high molecular weight polymers, such as proteins, pectins and others. Often they contribute significantly to the structure and viscosity of foods. In dilute solutions, the polymer chains are separate, and the intrinsic viscosity, denoted as $[\eta]$, of a polymer in solution depends only on the dimensions of the polymer chain. Because $[\eta]$ indicates the hydrodynamic volume of the polymer molecule and is related to the molecular weight and to the radius of gyration, it reflects important molecular characteristics of a biopolymer [Anandha, 1999]. It is straightforward to obtain the viscosity of a polymer solution in a simple U-tube viscometer where the time is measured for a known volume of solution to flow through a capillary tube [Bodanecky and Kovar, 1982].Simpler technique for determining the hydrodynamic radius is viscosimetry. Generally, the suspension of colloids or the dissolution of polymers leads to an increase in the measured

macroscopic viscosity. It is easy to see the principal reason for this effect when considering the simple shear flow [Gert, 2007].

A polymer is a very large molecule. A polymer molecule may be thousands or even millions of times larger than nonpolymer molecules [Madeline, 2004]. The use of polymer composites has grown at a phenomenal rate since the 1960s, and these materials now have an impressive and diverse range of applications in aircraft, spacecraft, boats, ships, automobiles, civil infrastructure, sporting goods and consumer products. The use of composites will continue to grow in coming years with emerging applications in large bridge structures, offshore platforms, engine machinery, computer hardware and biomedical devices ,although the use of composites is also substantial in the corrosion protection (eg. piping) [Mouritz and Gibson, 2006]. Polymer processing is defined as the “engineering activity” concerned with operations carried out on polymeric materials or systems to increase their utility [Bernhardt and Kelvey, 1958]. Primarily, it deals with the conversion of raw polymeric materials into finished products, involving not only shaping but also compounding and chemical reactions leading to macromolecular modifications and morphology stabilization, and thus, “value-added” structures.

Synthetically Modified Polysaccharides: Water solubility can be conferred on a number of naturally occurring polysaccharides by synthetic derivations producing charged or polar functionality. Two of nature’s most abundant polysaccharides, cellulose and chitin, have been synthetically modified in a multitude of ways to produce polymers with significant commercial utilization [Nevell and Zeronian, 1985; Lochhead, 1993].

Cellulose Derivatives: Cellulose is a β -1 \rightarrow 4-D-anhydroglucopyranosecopolymer as shown below that serves as the major structural component of plants.



When the cellulose molecule is extended, it is a flat ribbon with hydroxyl groups protruding laterally and is capable of forming both intra- and intermolecular hydrogen bonds. This form allows the strong interaction with neighboring chains that makes dissolution difficult. In fact, strongly interactive solvents are necessary for solubilization. Molecular weights range from 5×10^5 to 1.5×10^6 , depending on the source [Brant and Buliga, 1985].

Carboxymethyl cellulose (CMC) The common name for a cellulose ether of glycolic acid. It is an acid ether derivative of cellulose formed by the reaction of alkali cellulose with chloroacetic acid. It is usually marketed as a water-soluble sodium salt, more properly called sodium carboxymethyl cellulose. The sodium salt of this compound is commonly used as a stabilizer or an emulsifier. In the early literature, it is sometimes called cellulose glycolate or cellulose glycolic acid [Jan, 2007]. Carboxymethyl cellulose (CMC) is usually prepared by the reaction of cellulose with the sodium salt of chloroacetic acid in aqueous alkaline organic slurries. The extent of substitution on C-2, C-3, and C-6 is related to the degree of disruption of hydrogen bonding, steric factors, and reaction conditions [Brant and Buliga, 1985; Lochhead, 1993]. The acid form of CMC is a

polyelectrolyte with limited solubility and a PH of 4. The monovalent metal or ammonium salts are soluble; divalent cations result in borderline solubility; multivalent cations allow gel formation. Solutions of sodium CMC are pseudoplastic for high viscosity grades with degrees of substitution (DS) of 0.9–1.2. Solutions of less uniformly substituted, high molecular weight CMC with low DS are thixotropic; CMC is stable over the pH range 4–10. CMC is used in sizing for textile and paper applications and as a thickener, stabilizer, suspending agent, or binder in foods, pharmaceuticals, and cosmetics. CMC is a fluid loss and rheology modifier in drilling muds [Cormick, 2005]. CMC has the following structure:

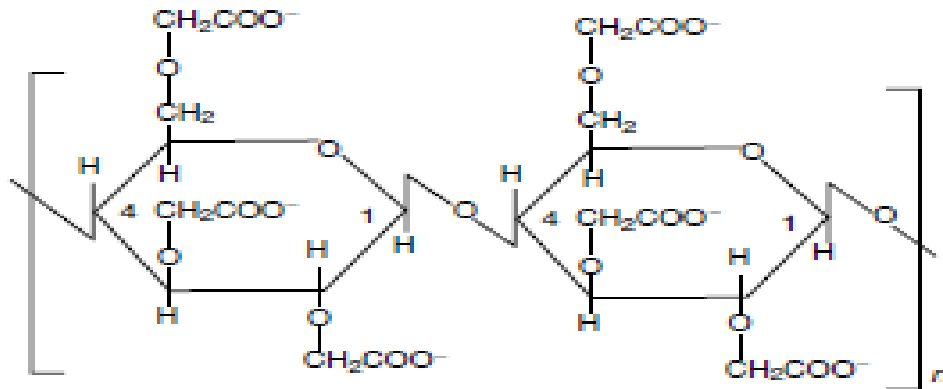


Figure 1-1: Chemical structure of CMC [James, 2007].

The aim of present work is to measure the intrinsic viscosity of five grads of carboxymethyl cellulose, determine the molecular weight of each grade, determine the value of critical molecular weight, determine the value of network parameters, and describe the behavior of carboxymethyl cellulose solution and compare with other polymer solution.

CHAPTER TWO

LITERATURE SURVEY

2.1 Polysaccharide

A variety of polysaccharides are generated by microorganisms. Examples include alginate, curdlane, dextran, gellan, glucan, pullulan, and xanthan. Also cellulose can be produced by microbes. Among the microbial polysaccharides, xanthan plays a dominant role due to the relative easiness to produce it and as a result of its outstanding properties. Indeed, it has found widespread applications ranging from food and cosmetics additives to enhanced oil recovery.

The xanthan polymer consists of repeated units of five sugars, namely, two D-glucose, two D-mannose, and one D-glucuronate, and varying amounts of acetate and pyruvate. Its primary structure is shown in Figure 2-1 based on the results of [Jansson 1975], and [Melton 1976], revised according to [Hassler Doherty 1990], and confirmed by [McIntyre 1996].

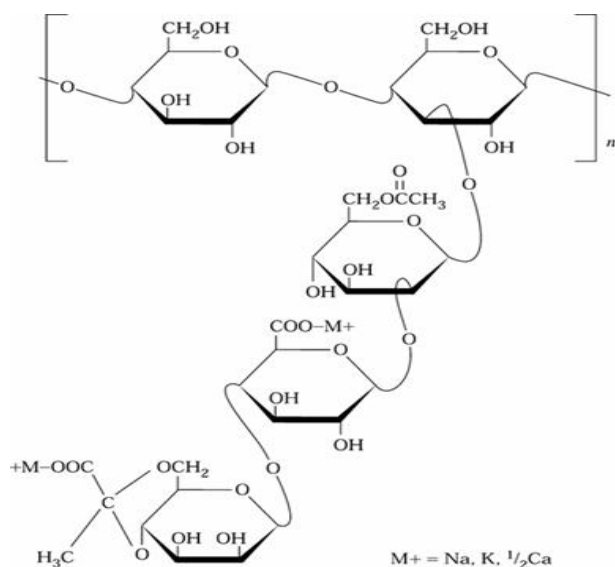


Figure 2-1: chemical structure of xanthan repeating unit

The polysaccharide backbone, made up of β -[1–4]-linked D-glucose units, is identical to that of cellulose. To alternate D-glucose units at the O–3 position, a trisaccharide side chain containing a D-glucuronosyl unit between two D-mannosyl units is attached. The terminal β -D-mannosyl unit is glycosidically linked to the O-4 position of the β -D-glucuronosyl unit, which in turn is glycosidically linked to the O-2 position of an α -D-mannosyl unit. The terminal α -D-mannosyl unit of the side chain contains a pyruvic acid moiety as a 4,6-cyclic acetal in variable degree. Finally, the nonterminal α -D-mannosyl unit is stoichiometrically substituted at O-6 with an acetyl group. Xanthan gum also contains monovalent cations, which can be Na, K, or $\frac{1}{2}$ Ca.

The secondary structure is known to undergo an order–disorder conformational transition at particular salinity and temperature levels, depending on the extent of pyruvate substitution [Clarke 1986], [Muller 1984]. Most authors explain the stabilization of the ordered form by a noncovalent packing of the side chains along the backbone by H-bonding. X-ray fiber studies have indicated that the polymer adopts a right-handed helical conformation with fivefold symmetry and a helix pitch of 4.7 nm³ [Moorhouse 1976]. However, the question of whether this polymer dissolves in water as a single [Moorhouse 1976] [Muller 1986] or a double strand [Holzward 1977], [Holzward 1978] has been a matter of controversial discussion. It now seems to be anticipated that xanthan may effectively be a single or a double strand, depending on the fermentation process, the acyl content, the thermal history, and the downstream process [Muller 1986], [Shatwell 1990], [Milas 1996].

The most important property of xanthan is its ability to form solutions of high viscosity at rest or at low shear forces, which are highly pseudoplastic, and may display also a viscosity yield value. The viscosity of xanthan solutions is stable over a wide range of salt concentrations (up to 150 g/L NaCl), temperature (up to 90 °C) and pH (2-11).

These solution characteristics of xanthan give rise to the functional properties such as thickening and stabilizing ability, which are used in a diverse range of applications.

In addition, xanthan shows a synergistic interaction with various galactomannans [Shatwell 1991], chitosan [Kumagai 1996], and β -lactoglobulin [Zasykin 1996], which results in enhanced solution viscosity or formation of gels, depending upon the type of mixture. The polysaccharide is prepared by inoculating a sterile aqueous solution of carbohydrate(s), a source of nitrogen, di-potassium monohydrogen phosphate, and some trace elements. The medium is well-aerated and stirred, and the polymer is produced extracellularly into the medium. The final concentration of xanthan produced is about three to five percent by weight. After fermentation over about four days, the polymer is precipitated from the medium by the addition of isopropyl alcohol and dried and milled to give a powder that is readily soluble in water or brine.

2.1.1 Commercial Applications

a- Food uses

Several applications that illustrate xanthan use in the food industry are given in Table 5. First of all xanthan gum is incorporated into foods to control the rheology of the final product. In performing this functional task, the polymer has a major effect on various sensory properties such as texture, flavor release, and appearance, which contribute to the acceptability of the product for consumer use. Because of its solution properties, xanthan can be used to provide a desired functionality at a

lower concentration than most gums and, therefore, may be more cost-effective. Additionally, because of its pseudoplastic properties in solution, xanthan has a less “gummy” mouth-feel than gums that exhibit Newtonian behavior. An additional advantage in food formulations is the antioxidative action of xanthan as compared with other polysaccharides and additives [Shimada 1996]. Xanthan is also being used in the formulation of reduced-calorie products, representing the second and third generation of fat replacers and stabilizers [Fryer 1996].

Table 2-1. Main Practical Uses of Xanthan for the Food Industry

Function	Application
Adhesive	Icings and glazes
Binding agent	Pet foods
Coating	Confectionery
Emulsifying agent	Salad dressing
Encapsulation	Powdered flavors
Film formation	Protective coatings, sausage casings
Foam stabilizer	Beer
Gluten substitution and dough processing	Baked goods, pasta

Stabilizer	Ice cream, salad dressings, juice drinks, margarine
Swelling agent	Processed meat products
Syneresis inhibitor, freeze–thaw stability	Cheese, frozen foods
Thickening agent	Jams, sauces, syrups, and pie fillings
Pumping and filling improvement	Processing of canned products

b- Cosmetics and Pharmaceutical Uses

Xanthan gum is used in cosmetics and toiletries as a bodying agent and emulsifier. Personal care products such as shampoos, creams, lotions, make-up, hair care products, and toothpastes can be formulated with xanthan [kang 1993], [B. C. C. 1994], [H. H. & P. P. I. 1996]. Additionally, xanthan provides creams and lotions with a good “skin-feel” during and subsequent to application [kang 1993]. Recently, a new xanthan formulation (Ticaxan) was introduced into the market for that purpose [H. H. & P. P. I. 1996].

In the pharmaceutical industry, xanthan is used to suspend pharmaceuticals such as antibiotics and to provide formulations of uniform

dosage [kang 1993]. It can also be used to stabilize emulsified cream formulations containing pharmaceuticals. Presently, xanthan is being evaluated in controlled-release applications, such as in gastrointestinal pharmaceutical applications, as rate limiting membranes for sustained delivery of oral formulations [Sujjaareevath 1997], [Roy 1996] and as dissolution and binding agents in tablets and rectal preparations [Ntawukulliyayo 1996], [Kondo 1996].

c- Agricultural and Other Industrial Applications

Xanthan is used in a diverse range of industrial applications, particularly as a suspending or thickening agent. The polymer improves the flowability of fungicides, herbicides, and insecticides by uniformly suspending the solid components of the formulation in an aqueous system or by stabilizing emulsions and multiphase liquid systems [kang 1993]. The unique rheological properties of xanthan solutions also improve sprayability, reduce drift, and increase pesticide cling and permanence [Pat 1973], [Pat 1972], [B. C. C. 1994]. Recently, various “tolerance exemptions” were issued by the U.S. Environmental Protection Agency for the use of xanthan as a surfactant in pesticide formulations [F. C. N. 1996]. Because of its ability to disperse and hydrate rapidly, xanthan is used in jet injection printing. It is nonpolluting and gives a good color yield. It is also used in several mining processes for removing dissolved metals in a highly efficient process [B. C. C. 1996]. Lately, in the formulation of a new generation of thermoset coatings, xanthan was introduced by Monsanto with the aim of addressing customers' environmental challenges [T. R. S. O. C. 1996].

d- Petroleum Industry

In the petroleum industry, xanthan gum finds a wide range of applications. Among these are oil drilling, fracturing, pipeline cleaning, workover, and completion. Xanthan's unique solution rheology, its excellent compatibility with salts, and its resistance to thermal degradation have made it useful as an additive to drilling fluids [kang 1993], [eur pat 1994]. The pseudoplasticity of its solutions provides low viscosity at the drill bit, where shear is high, and high viscosity in the annulus, where shear is low. Therefore, xanthan serves a dual purpose in allowing faster penetration at the bit because of the low solution viscosity in that area and, at the same time, suspending cuttings in the annulus because of the high solution viscosity in that area. Hydraulic fracturing is used to effect deep-penetrating reservoir fractures that improve productivity of the well. Xanthan's high solution viscosity at low shear is important for proppant suspension in this operation [u.s. pat 1994]. The pseudoplastic rheology, shear stability, and friction reduction imparted by xanthan provide for maximum delivery of pressure to the formation and minimal friction loss in the tubing and reservoir. A workover and completion fluid is essential for achieving and maintaining maximum well productivity. Xanthan contributes to excellent hole cleaning, suspension, friction reduction, and stability to shear and high temperatures. An important speciality

application employs a xanthan gel to remove rust, welding rods, wet slag, and other debris from gas pipelines. This pipeline cleaning method is considered safe, environmentally acceptable for open sea disposal, and cost-effective [kang 1993].

e- Enhanced Oil Recovery

For every barrel of oil actually produced, about another two remain in the ground [Gabriel 1979]. Therefore, enhanced oil recovery (EOR) may become important in the next decades to meet the increasing energy demand of the future. Xanthan gum can be used in two types of enhanced recovery systems. The principal use is for an improved form of water flooding in secondary oil recovery, a phase in which polymers are used to increase the efficiency of water contact and to displace reservoir oil. The second application is in micellar-polymer flooding as a tertiary oil recovery operation. Polymer-thickened brine is used to drive a slug of surfactant through the porous reservoir rock to mobilize residual oil; the polymer prevents fingering of the drive water through the surfactant bank and ensures good area sweep. In both applications, the function of the polymer is to reduce the mobility of injected water by increasing its viscosity. Evaluation of hundreds of biopolymers has found xanthan to be one of the best candidates for use in EOR operations. The reasons for this are its (1) non-Newtonian behavior, (2) high viscosity yield even at low concentrations (600–2,000 ppm), (3) low sensitivity of viscosity to salinity changes (unlike the polyacrylamides), (4) resistance to mechanical degradation, (5) stability with respect to higher temperature (up to almost 90 °C).

2.2 Rheology

Rheology can be classified into four types and they are:

1. Continuum rheology: The rheology that treats a material as a continuum without explicit consideration of microstructure. Also called macro rheology and phenomenological rheology [Barnes and Hutton, 1989].
2. Structure rheology: is to find the relationship between rheological measurements and the structure of the system [Gruber et. al., 1988].
- Rheometry: is the measuring arm of rheology and its basic function is to quantify the rheological material parameters of practical importance. A rheometer is an instrument for measuring the rheological properties and can do one of the following two things [Aron, 1999]:
 - a) It can apply a deformation mode to the material and measure the subsequent force generated, or
 - b) It can apply a force mode to a material and measure the subsequent deformation.
- Applied rheology: is concerned with the characterizing of various fluids encountered in chemical industries [Fredrickson, 1964].

2.3 Types Of Polymer Solution

Polymer solutions are important for a variety of purposes. For polymer solution it has been found useful to distinguish two regions [Schurze, 1991]:

1. The region of the particle solution (dilute solution).
2. The region of the network solution (concentrated solution).

2.3.1 The Particle Solution (Dilute-Solution)

This reign will be found at very low concentration it is the range of the intrinsic viscosity $[\eta]$ (limiting viscosity number) which describes the rheological behavior of this system [Schurze, 1996].

- 1) A catchall term that can mean any of the interrelated and quantitatively defined viscosity ratios of dilute polymer solutions or their absolute viscosities.
- 2) The kinematic viscosity of a solution as measured by timing the rate of efflux of a known volume of solution, by gravity flow, through a calibrated glass capillary that is immersed in a temperature-controlled bath. Two common types of viscometer are the Ostwald–Fenske and Ubbelohde. From the viscosities of the solution η and the solvent η' , and the solution concentration c , five frequently mentioned “viscosities” (viscosity ratios, actually) can be derived, as follows:

Relative viscosity: $\eta_r = \eta/\eta'$

Specific viscosity: $\eta_{sp} = \eta_r - 1$

Reduced viscosity: $\eta_{red} = \eta_{sp}/c$

Inherent viscosity: $\eta_{inh} = (\ln \eta_r)/c$

Intrinsic viscosity: $[\eta] =$ the limit as $c \rightarrow 0$ of η_{sp}/c , the limit as $c \rightarrow 0$ of η_{inh} .

The intrinsic viscosity, because it is extrapolated to zero concentration from a series of measurements made at different concentrations, is independent of concentration. However, different solvents yield

different intrinsic viscosities with the same polymer, so the solvent used must be identified [Jan, 2007].

Intrinsic Viscosity

Both the colligative and the scattering methods result in absolute molecular weights; that is, the molecular weight can be calculated directly from first principles based on theory. Frequently these methods are slow, and sometimes expensive. In order to handle large numbers of samples, especially on a routine basis, rapid, inexpensive methods are required.

Intrinsic viscosity measurements are carried out in dilute solution and

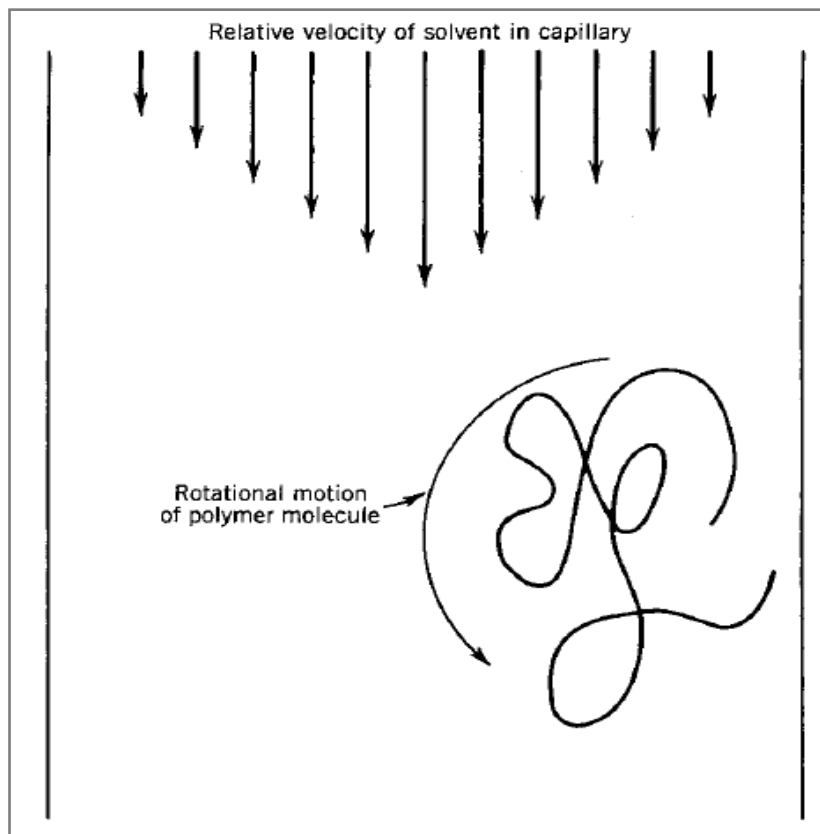


Figure 2-2: The effect of shear rates on polymer chain rotation. [Sperling, 2006].

result in the viscosity-average molecular weight. Consider such a dilute solution flowing down a capillary tube Fig.2-1. The flow rate, and hence the shear rate, is different depending on the distance from the edge of the capillary [Sperling, 2006]. The polymer molecule, although small, is of finite size and “sees” a different shear rate in different parts of its coil. This change in shear rate results in an increase in the frictional drag and rotational forces on the molecule, yielding the mechanism of viscosity increase by the polymer in the solution [Sperling, 2006].

Definition of Terms

The solvent viscosity is η_s , usually expressed in poises, Stokes, or, more recently, Pascal seconds, Pa.s. The viscosity of the polymer solution is η . The relative viscosity is the ratio of the two:

$$\eta_{rel} = \frac{\eta}{\eta_s} \quad \dots (2.1)$$

where η_s is the viscosity of the solvent.

The relative viscosity is a quantity larger than unity. The specific viscosity is the relative viscosity minus one:

$$\eta_{sp} = \eta_{rel} - 1 \quad \dots (2.2)$$

Usually η_{sp} is a quantity between 0.2 and 0.6 for the best results. The specific viscosity divided by the concentration and extrapolated to zero concentration, yields the intrinsic viscosity:

$$\left[\frac{\eta_{sp}}{c} \right]_{c=0} = [\eta] \quad \dots (2.3)$$

For dilute solutions, where the relative viscosity is just over unity, the following algebraic expansion is useful:

$$\ln \eta_{rel} = \ln(\eta_{sp} + 1) \cong \eta_{sp} - \frac{\eta_{sp}^2}{2} + \dots \quad \dots (2.4)$$

Then, dividing $\ln \eta_{rel}$ by c and extrapolating to zero concentration also yields the intrinsic viscosity:

$$\left[\frac{\ln \eta_{rel}}{c} \right]_{c=0} = [\eta] \quad \dots (2.5)$$

Note that the natural logarithm of η_{rel} is divided by c in equation (2.5), not η_{rel} itself. The term $(\ln \eta_{rel})/c$ is called the *inherent viscosity*. Also note that the intrinsic viscosity is written with h enclosed in brackets. This is not to be confused with the plain h, which is used to indicate solution or melt viscosities [Sperling, 2006].

Two sets of units are in use for $[\eta]$. The “American” units are 100 cm³/g, whereas the “European” units are cm³/g. Of course, this results in a factor of 100 differences in the numerical result. Lately, the European units are becoming preferred [Sperling, 2006].

The Equivalent Sphere Model

In assuming a dilute dispersion of uniform, rigid, no interacting spheres, Einstein [Levine et. al., 1979; Pantelis and Davies, 1988] derived an equation expressing the increase in viscosity of the dispersion:

$$\eta = \eta_s(1 + 2.5v_2) \quad \dots (2.6)$$

where the quantity v_2 represents the volume fraction of spheres. The intrinsic viscosity of a dispersion of Einstein spheres is 2.5 for v_2 , or 0.025 for concentration in units of g/100 cm³.

Now consider a coiled polymer molecule as being impenetrable to solvent in the first approximation. Hydrodynamic spheres of equivalent radius Re will be used to approximate the coil dimensions

see Fig. 2-2. In shear flow, it exhibits a frictional coefficient of f_o . Then according to Stokes law as shown in Eq. (2.7):

$$f_o = 6\pi_1\eta_s R_e \quad \dots (2.7)$$

where R_e remains quantitatively undefined.

The Einstein viscosity relationship for spheres may be written:

$$\frac{\eta - \eta_s}{\eta_s} = \eta_{sp} = 2.5 \left(\frac{n_2}{V} \right) V_e \quad \dots (2.7)$$

Where n_2/V is the number of molecules per unit volume, $V_e = \left(\frac{4\pi}{3} \right) R_e^3$.

The quantity $n_2 V_e / V$ is the volume fraction of equivalent spheres, yielding the familiar result that the viscosity of an assembly of spheres is independent of the size of the spheres, depending only on

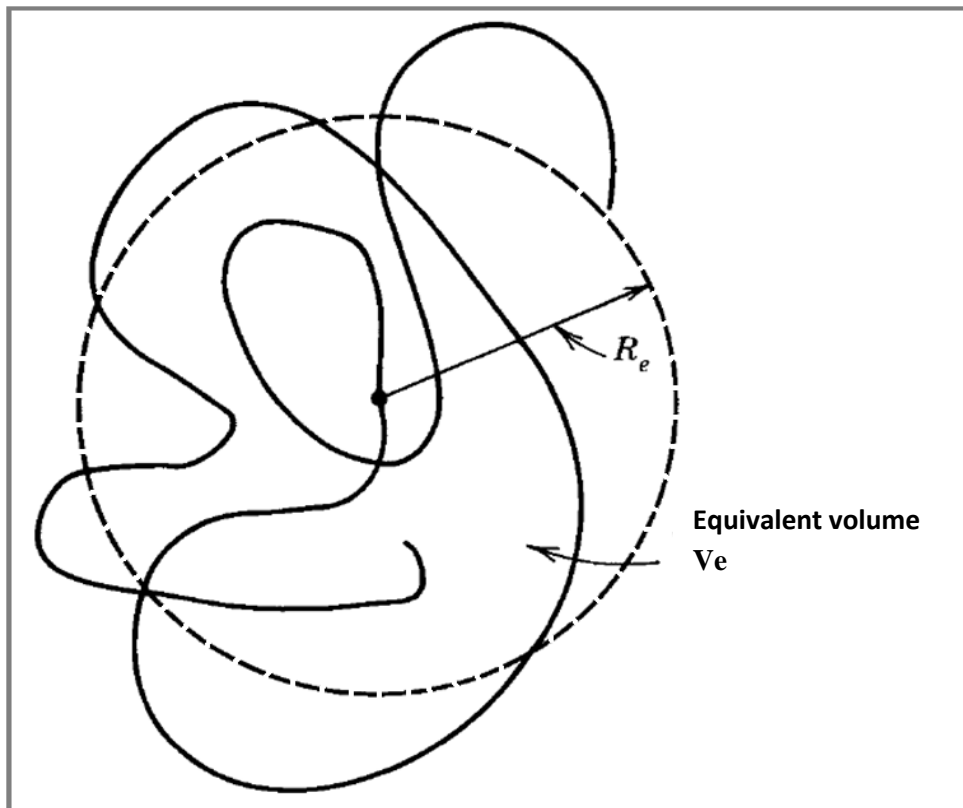


Figure 2-3: The equivalent sphere model [Sperling, 2006].

their volume fraction.

$$\frac{n_2}{V} = \frac{cN_A}{M} \quad \dots (2.8)$$

where c is the concentration and N_A is Avogadro's number,

$$\left[\frac{\eta_{sp}}{c} \right]_{c=0} = [\eta] = 2.5 \frac{N_A V_e}{M} \quad \dots (2.9)$$

Note that

$$\frac{V_e}{M} = \frac{4\pi_1 R_e^3}{3 M} = \frac{4\pi_1}{3} \left(\frac{R_{e0}^2}{M} \right)^{3/2} M^{1/2} \quad \dots (2.10)$$

and

$$R_e = R_{e0} \alpha \quad \dots (2.11)$$

where α is the expansion of the coil in a good solvent over that of a Flory θ -solvent [Sperling, 2006].

The quantity R_{e0}^2/M is roughly constant. The same constant appears in Brownian motion statistics, where time takes the place of the molecular weight. This expresses the distance traveled by the chain in a random walk as a function of molecular weight. According to Flory [Schiraldi et. al., 1996], the expansion of the coil increases with molecular weight for high molecular weights as $M^{0.1}$, yielding

$$[\eta] = 2.5 \frac{4\pi_1}{3} N_A \left(\frac{R_{e0}^2}{M} \right) M^{1/2} \alpha^3 \quad \dots (2.12)$$

The Mark–Houwink–Sakurada Relationship

In the late 1930s and 1940s Mark, Houwink, and Sakurada arrived at an empirical relationship between the molecular weight and the intrinsic viscosity [Breene et. al., 1990]:

$$[\eta] = K M_v^a \quad \dots (2.13)$$

where K and a are constants for a particular polymer–solvent pair at a particular temperature. Equation (2.13) is known today as the Mark–

Houwink– Sakurada equation. This equation is in wide use today, being one of the most important relationships in polymer science and probably the single most important equation in the field [Eich et al.,1998]. It must be pointed out that since viscosity-average molecular weights are difficult to obtain directly, the weight-average molecular weights of sharp fractions or narrow molecular weight distributions are usually substituted to determine K and a .

According to equation (2.12) the value of α is predicted to vary from 0.5 for a Flory θ -solvent to about 0.8 in a thermodynamically good solvent. This corresponds to a increasing from a zero dependence on the molecular weight to 0.1 power dependence. More generally, it should be pointed out that a varies from 0 to 2; see Table (A.1) in appendix A.

The quantity K is often given in terms of the universal constant Φ ,

$$K = \Phi \left(\frac{\bar{r}_0^2}{M} \right)^{3/2} \quad \dots (2.14)$$

where \bar{r}_0^2 represents the mean square end-to-end distance of the unperturbed coil. If the number-average molecular weights are used, then Φ equals 2.5×10^{21} dl/mol·cm³. A theoretical value of 3.6×10^{21} dl/mol·cm³ can be calculated from a study of the chain frictional coefficients [Schiraldi et al., 1996]. For many theoretical purposes, it is convenient to express the Mark–Houwink–Sakurada equation in the form:

$$[\eta] = \Phi \left(\frac{\bar{r}_0^2}{M} \right)^{3/2} M^{1/2} \alpha^3 = KM^{1/2} \alpha^3 \quad \dots (2.15)$$

Note that a widely used older value of Φ is 2.1×10^{21} dl/mol·cm³.

If the intrinsic viscosity is determined in both a Flory θ -solvent and a “good” solvent, the expansion of the coil may be estimated. From equation (2.11):

$$[\eta]/[\eta]_{\theta} = \alpha^3 \quad \dots (2.16)$$

Values of α vary from unity in Flory θ -solvents to about 2 or 3, increasing with molecular weight.

Intrinsic Viscosity Experiments

In most experiments, dilute solutions of about 1% polymer are made up. The quantity η_{rel} should be about 1.6 for the highest concentration used. The most frequently used instrument is the Ubbelohde viscometer, which equalizes the pressure above and below the capillary [Spurling, 2006].

Several concentrations are run and plotted according to Fig.2-3.

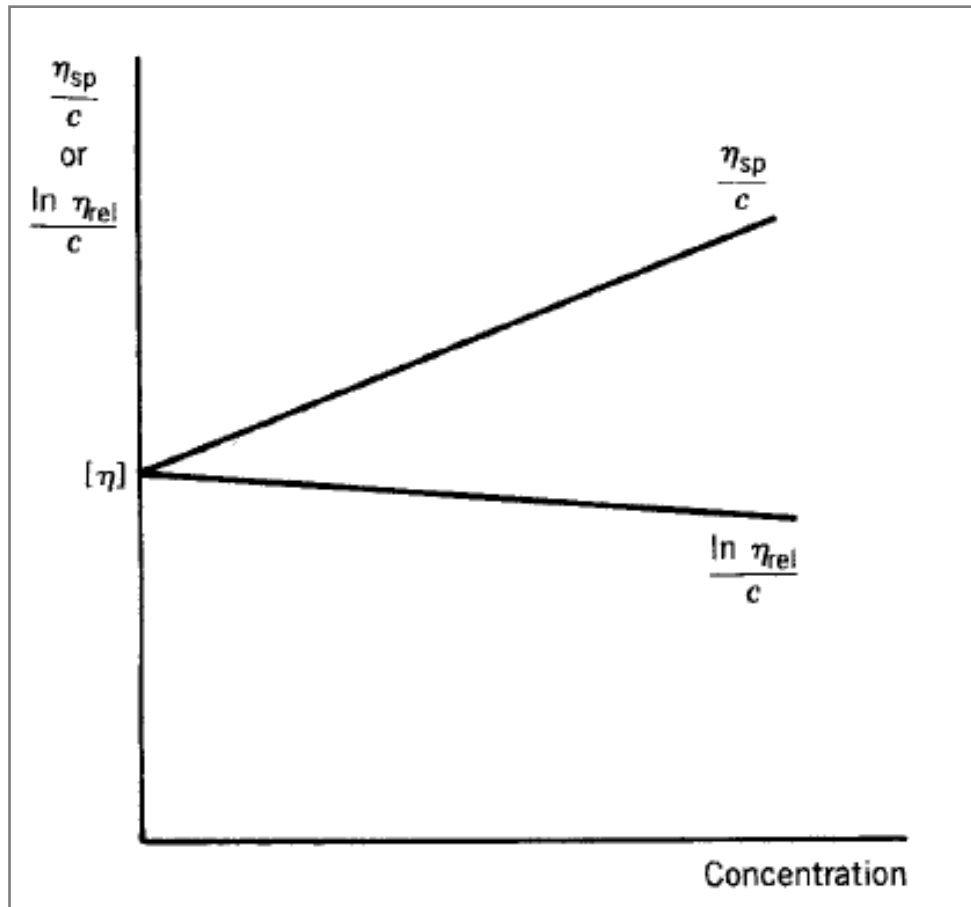


Figure 2-4: Schematic of a plot of η_{sp}/c and $\ln \eta_{rel}/c$ versus c , and extrapolation to zero concentration to determine $[\eta]$ [Sperling, 2006].

Two practical points must be noted:

- 1) Both lines must extrapolate to the same intercept at zero concentration.
- 2) The sum of the slopes of the two curves is related through the Huggins [Rao et. al., 1986, A] equation:

$$\frac{\eta_{sp}}{c} = [\eta] + k'[\eta]^2 c \quad \dots (2.17)$$

and the Kraemer [Rao et. al., 1986, B] equation:

$$\frac{\ln \eta_{rel}}{c} = [\eta] - k''[\eta]^2 c \quad \dots (2.18)$$

Algebraically

$$k' + k'' = 0.5 \quad \dots (2.19)$$

If either of these requirements is not met, molecular aggregation, ionic effects, or other problems may be indicated. For many polymer–solvent systems, k' is about 0.35, and k'' is about 0.15, although significant variation is possible.

Noting the negative sign in equation (2.18), k'' is actually a negative number.

The molecular weight is usually determined through light-scattering, as indicated previously. In order to determine the constants K and a in the Mark–Houwink–Sakurada equation, a double logarithmic plot of molecular weight versus intrinsic viscosity is prepared see Fig.2-4 [Garito, 1989]. Results of this type of experiment were used in compiling Table A.1 in appendix A.

While use of the viscosity-average molecular weight of a polymer in calibrating K and a in equation (2.13), M_V values usually are not initially known. The calibration problem may be alleviated by one or more of the following methods:

1. Use of fractionated polymers.
2. Use of polymers prepared with narrow molecular weight distributions, such as via anionic polymerization.

- Use of weight-average molecular weight of the polymer, since it is closer than the number-average molecular weight.

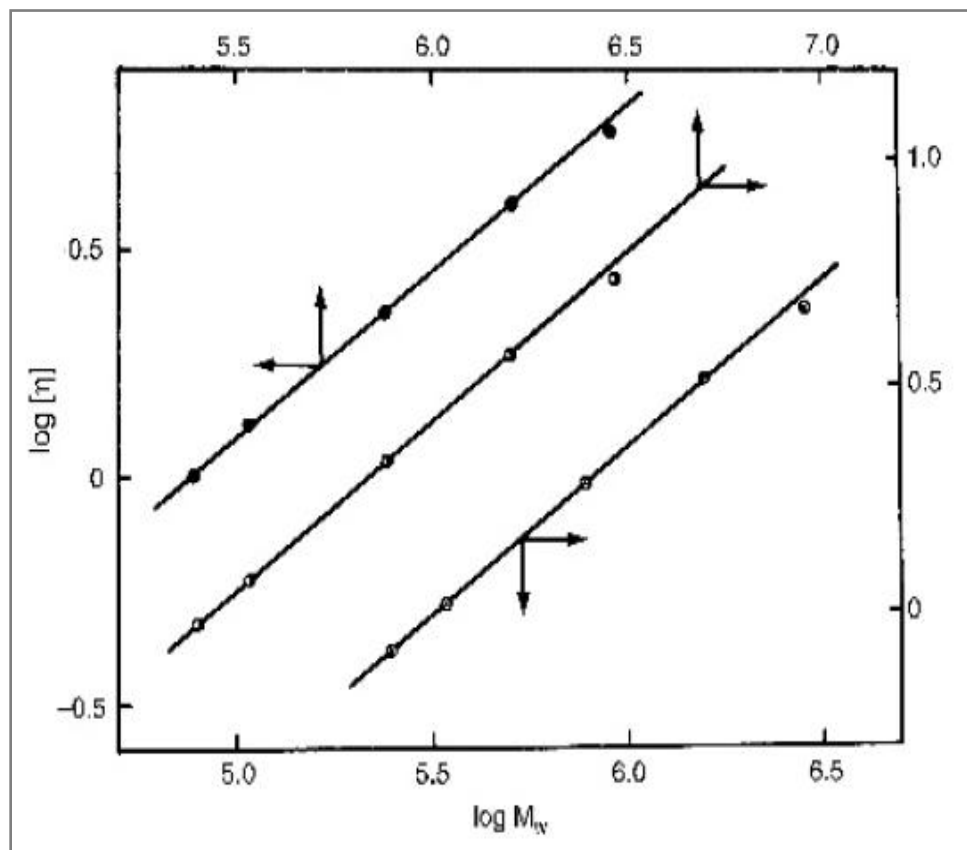


Figure 2-5: Double logarithmic plots of $[\eta]$ versus M_w for anionically synthesized polystyrenes, which were then fractionated leading to values of M_w/M_n of less than 1.06. Filled circles in benzene, half-filled circles in toluene, and open circles in dichloroethylene, all at 30°C. The arrows indicate the axes to be used. Units for $[\eta]$ in 100 ml/g [Garito, 1989].

2.3.2 The Network Solution (Semidilute and Concentrated-Solution)

In semidilute and concentrated solutions, polymer molecules are no longer isolated from one another. Chain–chain interactions at and above a critical concentration (c) often termed the overlap concentration, lead to increased values of apparent viscosity η . Apparent viscosity can be related to

concentration and molecular weight by equation 2.20, in which b and d are scaling constants.

$$\eta \propto c^b M^d \quad \dots (2.20)$$

Usually plots of $\ln \eta$ vs $\ln c$ at constant molecular weight (Fig. 2-5a) or $\ln \eta$ vs $\ln M$ at constant concentration (Fig. 2-5b) are used to measure entanglement onset. Measurements are made at constant shear rate, temperature, and solvent conditions [Cormick, 2005].

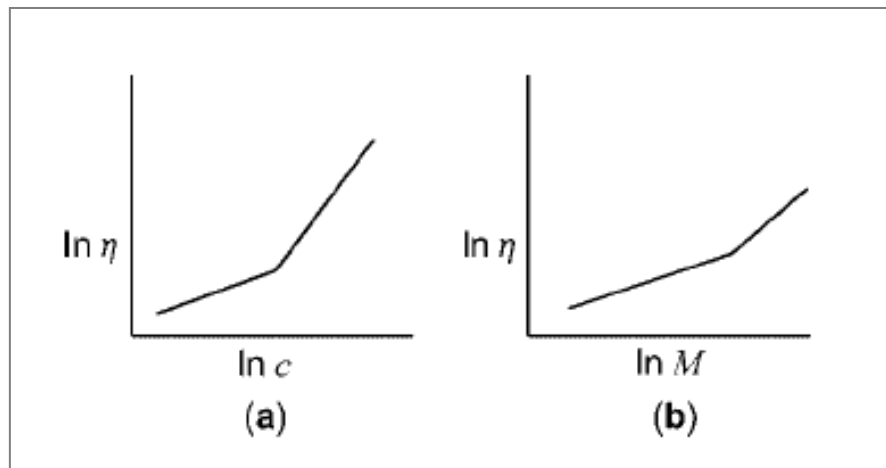


Figure 2-6: Relationship between apparent viscosity and (a) concentration at constant molecular weight; (b) molecular weight at constant concentration [Cormick, 2005].

Polymer chains in dilute solutions are isolated and interact with each other only during brief times of encounter. Increasing the polymer concentration in a solvent leads to a change at a certain stage. As is schematically indicated in Fig. 2-6, a limit is reached when the polymers molecules become closely packed because then they begin to interpenetrate [Sperling, 2006].

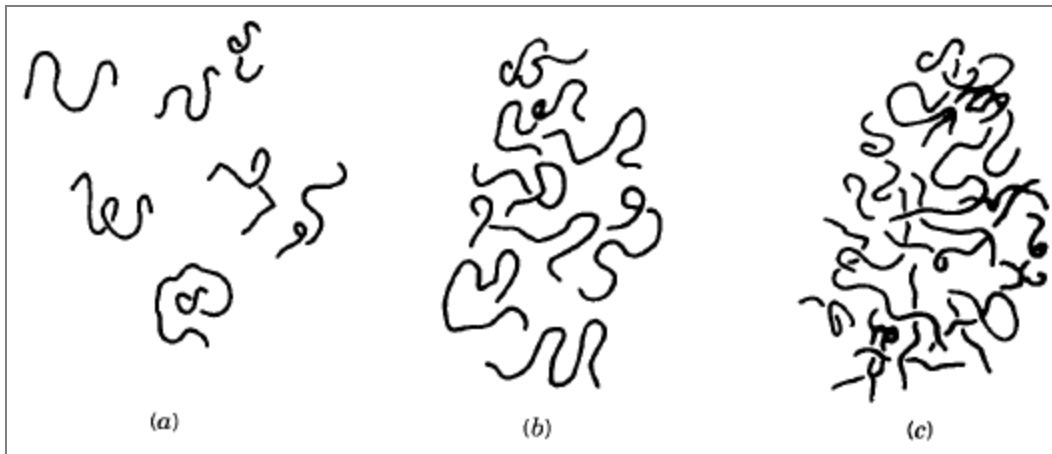


Figure 2-7: Relationships of polymer chains in solution at different concentration regions. (a) Dilute solution regime (b) The transition regions, (c) Semi-dilute regime [Sperling, 2006].

For network solution we must use a different description since in this case no individual particles are present see Fig. 2-7.

The statistical chain element $A'(C)$ depends on the concentration, and its extrapolation to zero concentration yields the true statistical chain element $A'_0(C)$ as obtained in dilute solution.

The value of D_N , v , and $A'(C)$ can be calculated from M_e the molecular mass a network strand [Buche, 1962]. The entanglement density is the number of entanglement per unit volume; it can be obtained by the formula:

$$V = \frac{C \cdot N_L}{M_e} \quad \dots (2.21)$$

where N_L is the Avogadro's number

Kuhen [1950] has put forward his description of polymer coiling by an equivalent model based on the statistical chain element (A), by regarding a real chain consisting of (P), the degree of polymerization, repeating of mass m_0 (with $M=P \cdot m_0$) and length L_0 .

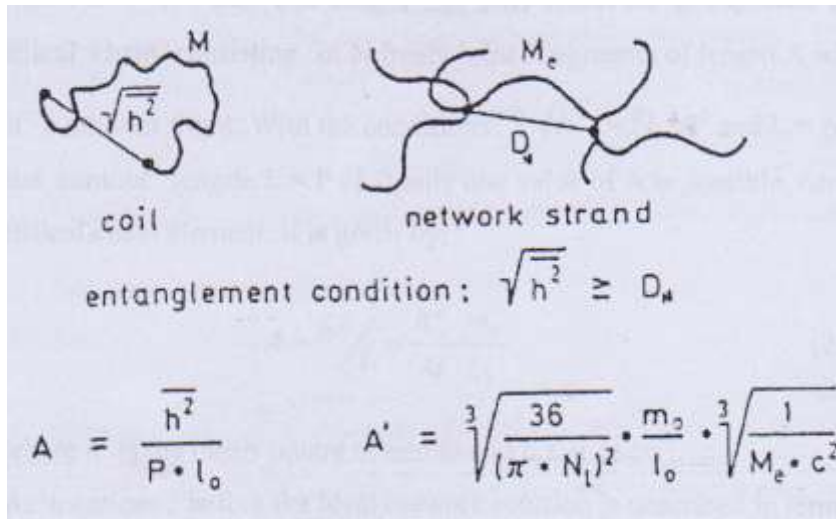


Figure 2-8: The chain element concept [Buche, 1962].

This molecules replaced by a hypothetical chain consisting of N freely joined segments of length A which perform a random flight. With the conditions $\bar{h}^2 = N \cdot A^2$ and $L = N \cdot A$ (L is the contour length, $L = P \cdot L_0$) only one value of A is possible, namely the statistical chain element. It is given by:

$$A = \frac{\bar{h}^2}{L} = \frac{\bar{h}^2 \cdot m_0}{M \cdot L_0} \quad \dots (2.22)$$

where \bar{h}^2 is the mean square of end to end distance of coil .

As mentioned before the ideal network solution described in term of an apparent statistical chain element $A'(C)$. This is obtained from measurement of M_e which is concentration dependent.

The network will be built if D_{coil}/D_N , the available volume for a coil is $(M/C \cdot N_L)$, but for an entanglement network, it is $(M_e/C \cdot N_L)$. At the same time a molecule as ball has a volume $(D_N \pi^3/6)$ which is equivalent volume and the statistical thread element $A'(C)$ is as:

$$A(C) = \frac{D_N^2}{L} \quad \dots (2.23)$$

$$\text{So equivalent volume} = \frac{\pi 1(A(c) \cdot L)^{3/2}}{6} \quad \dots (2.24)$$

By equating the two volumes:

$$\frac{\pi 1(A(c) \cdot L)^{3/2}}{6} = \frac{M_e}{C \cdot N_L} \quad \dots (2.25)$$

$$L = P \cdot L_o = \frac{M_e}{m_o} \cdot L_o \quad \dots (2.26)$$

Substituting equation 2.26 in to equation 2.25 yields:

$$A(C) = \sqrt[3]{\frac{36}{(\pi 1 \cdot N_L)^2}} \cdot \left(\frac{m_o}{L_o}\right) \cdot \sqrt[3]{\frac{1}{M_e \cdot C^2}} \quad \dots (2.27)$$

By extrapolating A(C) to zero concentration, we obtained the true chain element A(0).

2.4 Review of Local Work In Al-Nahrain Univesity:

AL-Sa'aidy [1997] studied the rheological properties of Novolak–acetone solution. Novolak is a type of phenol formaldehyde resins. Five grades of novolak with different concentrations (0.02, 0.04, 0.06, 0.08, and 1 g/cm³) were employed to predict the properties of concentrated mixtures were also studied from concentration (0.6 to 0.8 g/cm³).

A rheological study on polyvinyl alcohol dissolved in water was undertaken by Sultan [1998]. Five grades of polyvinyl alcohol were used; four were pure grades and the fifth one was a mixture of two grades. The study involved structural analysis of polyvinyl alcohol solution and the dilute region with concentrations for each grade (0.20, 0.40, 0.60, 0.80, 1.00, and 1.20 g/dL), and in concentrated (network) region with six concentrations also (3.28, 4.10, 5.12, 6.4, 8, and 10 g/dL).

A rheological study was performed by Al-Dory [1999] using a solution of polyethylene glycol – water. First the properties of a dilute solution were measured by using six concentrations of five grades of polyethylene glycol (0.04, 0.06, 0.08, 0.10, 0.12, and 0.14 g/ml). Then the network solution properties were studied in three concentration (0.4, 0.6, and 0.8 g/ml) for each grade.

Salman [2000] studied rheological properties of polychloroprene of different molecular weights dissolved in toluene at different concentrations in two regions dilute and network. In dilute measured by using ten concentrations of five grades of polychloroprene (0.001, 0.002, 0.003, 0.004, 0.005, 0.006, 0.007, 0.008, 0.009, and 0.01gm/cm³). Then the network

solution properties were studied in three concentrations (0.3, 0.35, 0.4, 0.45, and 0.5 gm/cm³) for each grade.

Table 2-2: $[\eta]$ and Mv for Novolak in Acetone

Grade	$[\eta]$ ml/gm	Mwt
LN1	1.544	11,600
LN2	4.590	117,600
LN3	2.361	28,600
LN4	4.274	101,000
LN5	3.456	64,300

Table 2-3: $[\eta]$ and Mv for Polyvinyl alcohol in water.

Grade	$[\eta]$ ml/gm	Mwt
GL-05B	4.238	19,900
G2	6.965	53,900
M	8.280	76,200
GH-20	10.085	113,000
C&B	11.035	135,300

Table 2-4: $[\eta]$ and Mv for Polyethylen glycol in water

Grade	$[\eta]$ ml/gm	Mwt
PEG1	16.7078	6,000
PEG2	15.2461	5,000
PEG3	12.9600	4,000
PEG4	7.1187	1,500
PEG5	3.4550	400

Table 2-5: $[\eta]$ and Mv for polychloroprene in toluene

Grade	$[\eta]$ ml/gm	Mwt
NEO1	83.0664	7,400,000
NEO2	68.5637	5,300,000
NEO3	101.69	10,100,000
NEO4	141.591	12,600,000
NEO5	129.784	15,000,000

Conclusions from the Previous local Works

Rheological methods can be successfully employed especially the study of viscosity and its dependence on rate of shear of normal force, and of solution elasticity, such measurement allow a detailed characterization of the structure of the network.

The above studies on polymer solution were made on two parts, dilute and concentrated solutions. The dilute region involved the determination of the intrinsic viscosity $[\eta]$ was calculated for each grade and from it the molecular weight M_v was determined from Mark – Houwink equation.

The concentrated region involved the determination of the network parameters (M_e , $A(C)$, V , D_N), where a plot of η_0 versus M_v was produced to determine the above parameters, the other parameter were calculated according to special relationships.

CHAPTER THREE

EXPERIMENTAL WORK

3.1 Materials

1. Five samples of Carboxymethyl cellulose (CMC), with different molecular weight, were supplied by Vegetable Oil Co./ Baghdad. And the CMC property: white to creamy, odourless , nontoxic, water-soluble.
2. NaOH solid pellet available in Vegetable Oil Co.
3. Water was distilled in the laboratory of Vegetable Oil Co.

6% NaOH in H₂O (as solvent) was prepared in the laboratory by weighting 6 gm of NaOH then complete the valume to 100 ml of water.

3.2 Preparation of solutions:

For the five grades of Carboxymethyl cellulose, dilute solutions were prepared. The first concentration (0.1%) was prepared by weighting ≈ 0.1 gm of CMC and this quantity was put in the beaker flask of 200 ml. then the volume of the beaker flask was completed with 6% NaOH in H₂O to 100 ml. The water bath has been kept at a constant temperature of 25 °C. At the first, the viscometer was cleaned and refilled with fresh solvent before measuring the flow time and dried with a stream of hot air.

Concentrated solutions of 0.01, 0.02, 0.03 and 0.04 gm/cm³ of CMC samples have been used. The 0.01 gm/cm³ solution was prepared, as example, by weighing 1 gm of CMC and placed in beaker, and then the volume has been completed with the solvent to 100 ml.

After the concentrations 0.01, 0.02, 0.03, and 0.04 gm/cm³ were prepared; they have been allowed 72 hours to dissolve completely.

3.3 Apparatus

1. Since intrinsic viscosity determination does not require the absolute η value, the BS/U-Tube Viscometer type (D) was used, figure (3-1).
2. The rotational viscometer (MYR S.L., vendrell, Spain, type: V1, Model: R) as shown in fig 3.2 was used for the concentrated solutions to determine the viscosity with different RPM, this instrument has eight rotational speeds (200, 100, 60, 50, 30, 20, 12, and 10 RPM).
3. Ten volumetric flasks with volume of 100 ml.
4. Pipette of 5ml.
5. Stop watch.
6. Thermometer.
7. Rubber tube.
8. Electronic balance of saunter type with accuracy .
9. Water bath with thermostat of Julabo HC type, with temperature control of 0.1 °C.
10. Magnetic stirrer with heater.

3.4 Measurements of Viscosity

3.4.1 Dilute solutions

Determinations of solution viscosity are achieved by comparing the efflux time (t) required for a specified volume of polymer solution to flow through a capillary tube with the corresponding efflux time (t_s) of the solvent. The usefulness of solution viscosity as a measure of polymer molecular weight

has been recognized ever since the early work of Staudinger (1930). The viscosity measurement had been used for the determination of the intrinsic viscosity [Sperling, 2006].

Intrinsic Viscosity

Intrinsic viscosity is known as the Staudinger index or limiting viscosity number [Gowariker et. al, 1987]. The intrinsic viscosity can be defined according to Hagen – Poiseuille law [Tveskov et. al, 1970]:

$$\eta = \frac{\pi P r^4 t}{8 V L} \quad \dots (3.1)$$

Assume a polymer solution is flowing through a capillary tube, the time required for the liquid of volume V to pass through the capillary of radius r and length L is t, where p is the pressure head under which the liquid flow takes place. Then:

$$t = \frac{8 V L \eta}{\pi P r^4} \quad \dots (3.2)$$

Equation (3.2) thus correlates the flow time with the absolute viscosity of liquid. If η and η_s are absolute viscosities of a solution and the pure solvent respectively, t and t_s are their corresponding flow time, the following relationships can be derived:

$$t = \left(\frac{8 V L}{\pi P r^4} \right) \eta \quad \dots (3.3)$$

$$t_s = \left(\frac{8 V L}{\pi P r^4} \right) \eta_s \quad \dots (3.4)$$

for the same capillary tube, the quantities within parenthesis have the same value; hence, dividing equation (3.3) by equation (3.4) gives:

$$\frac{t}{t_s} = \frac{\eta}{\eta_s} \quad \dots (3.5)$$

The term η/η_0 is known as the relative viscosity. This term and other terms related to viscosity measurement are given as follows:

$$\text{Relative viscosity} = \eta/\eta_s = t/t_s = \eta_{re}.$$

$$\text{Specific viscosity} = (\eta - \eta_s)/\eta_s = (t - t_s)/t_s = \eta_{re} - 1 = \eta_{sp}.$$

$$\text{Reduction viscosity} = \eta_{sp}/C = \eta_{red} \text{ cm}^3/\text{gm}.$$

$$\text{Intrinsic viscosity} = (\eta_{sp}/C)_{C \rightarrow 0} = [\eta] \text{ cm}^3/\text{gm}.$$

It may be noted from the above derivation, that for calculating the intrinsic viscosity of a polymer sample in solution, there is no need to know the absolute viscosity of a polymer sampler in solution, there is no need know the absolute viscosities of the solvents and the solutions, but only know the flow time of a constant volume of solvent and the solutions through a particular capillary tube. This principle is used in the viscometric technique of molecular weight determination.

Procedure of Measurement

The viscometer (see Fig. 3-1) was fastened, accurately vertical, in a water bath with controlled temperature. A and B are the timing marks, C is the filling mark. The solvent was allowed 10-15 minutes to reach the desired temperature. Then it has been sucked up into the timing bulb unit. It should reach few millimeters above mark A. The time

flow of the solution between mark A and B was determined with a stopwatch reading.

The readings have been repeated five times for each sample and the algebraic mean of this was taken to give the reading of each point.

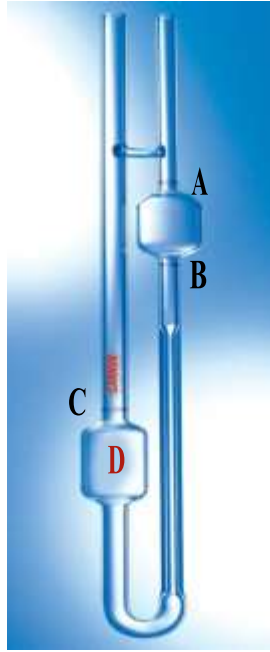


Figure 3-1:BS/U-Tube Viscometer type D

3.4.2 Concentrated solution

The spindle of the rotational viscometer has been immersed in the sample up to the immersed point, indicated with a groove on the same spindle. There are different types of spindle (G1, G2, G3, G4, G5, G6 and G7) for different range of viscosities; spindle type G2 and G3 have been chosen for the CMC solutions.

The spindle has been run in different RPM; the results were taken at the same time for each RPM and for each CMC solutions, all at fixed temperatures.

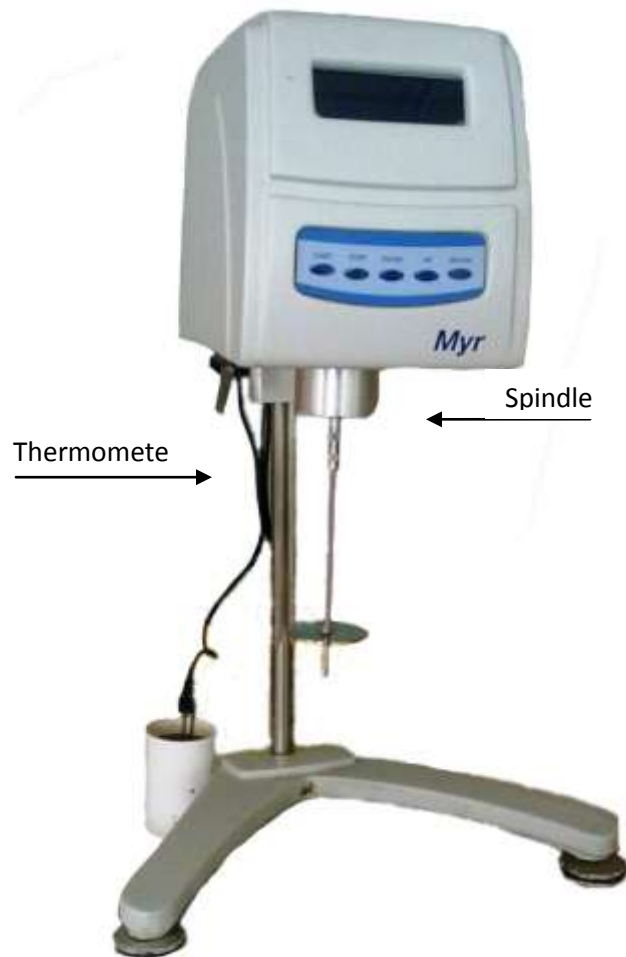


Figure 3-2: MYR Rotational Viscometer

CHAPTER FOUR

RESULTS AND DISCUSSION

4.1 Intrinsic Viscosity Calculation

The definition of intrinsic viscosity is given by:

$$[\eta] = (\eta_{sp}/C)_{C \rightarrow 0} \quad \dots (2.5)$$

$$\eta_{sp} = \frac{t_{solution} - t_{solvent}}{t_{solvent}} \quad \dots (4.1)$$

$$\eta_{red} = \eta_{sp}/c \quad \dots (4.2)$$

The results of time of flow with concentration for the seven grades of CMC, the specific viscosity ($\eta_{sp} = \frac{t_{solution} - t_{solvent}}{t_{solvent}}$), ($t_{solvent} = 15.57 \text{ sec}$), where the η_{sp} has been calculated for the seven grades and the reduction viscosity ($\eta_{red} = \eta_{sp}/c$) also calculated for each grades of CMC.

Note: the flow time in tables B-1 to B-5 in appendix is the average of five experimental readings for each point.

If the relation of concentration with reduction viscosity has been represented by graphs, Figs. 4-1 to 4-5 are obtained.

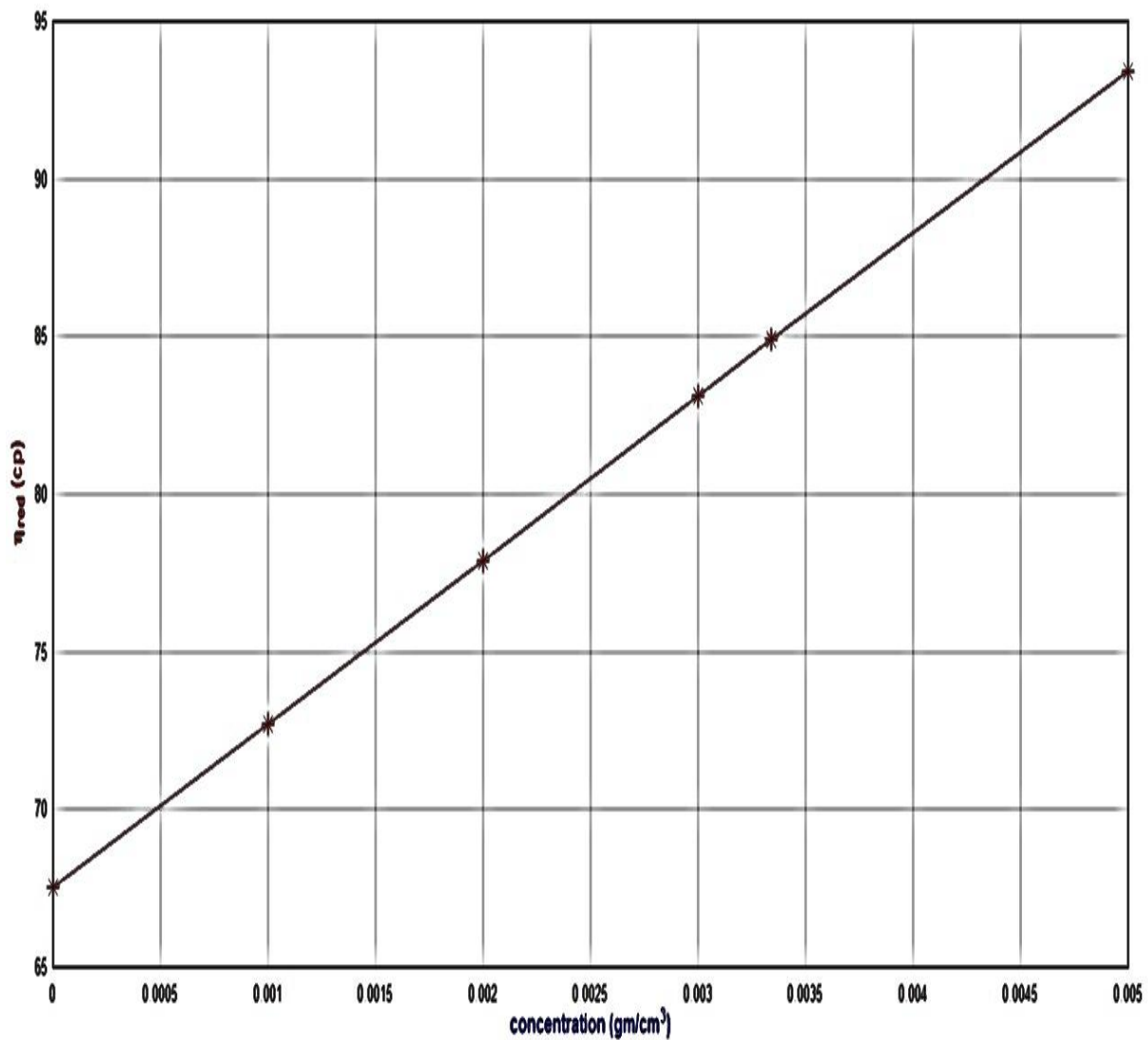


Figure 4.1: Relationship between concentration and reduction viscosity for CMC1.

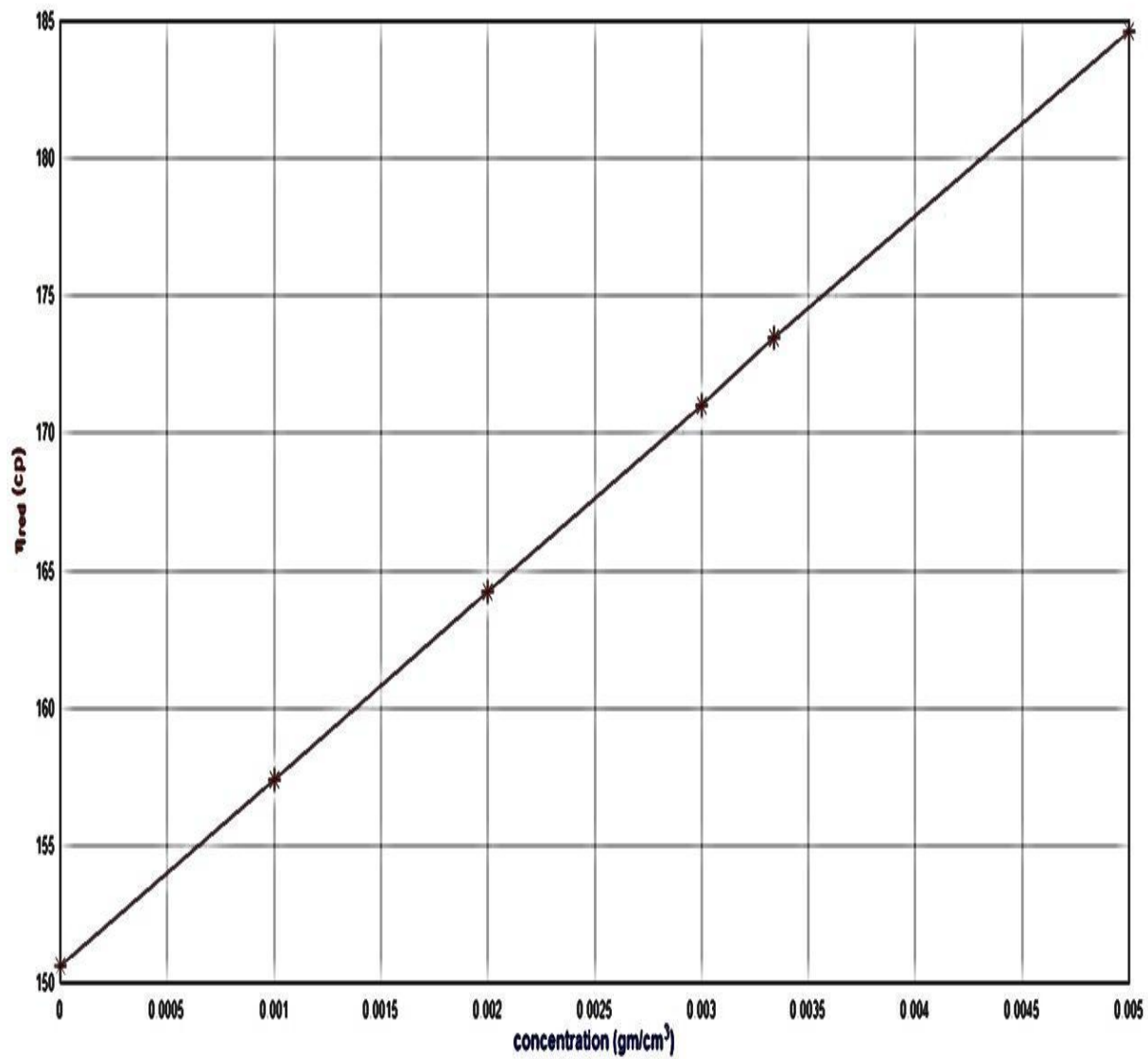


Figure 4.2: Relationship between concentration and reduction viscosity for CMC2.

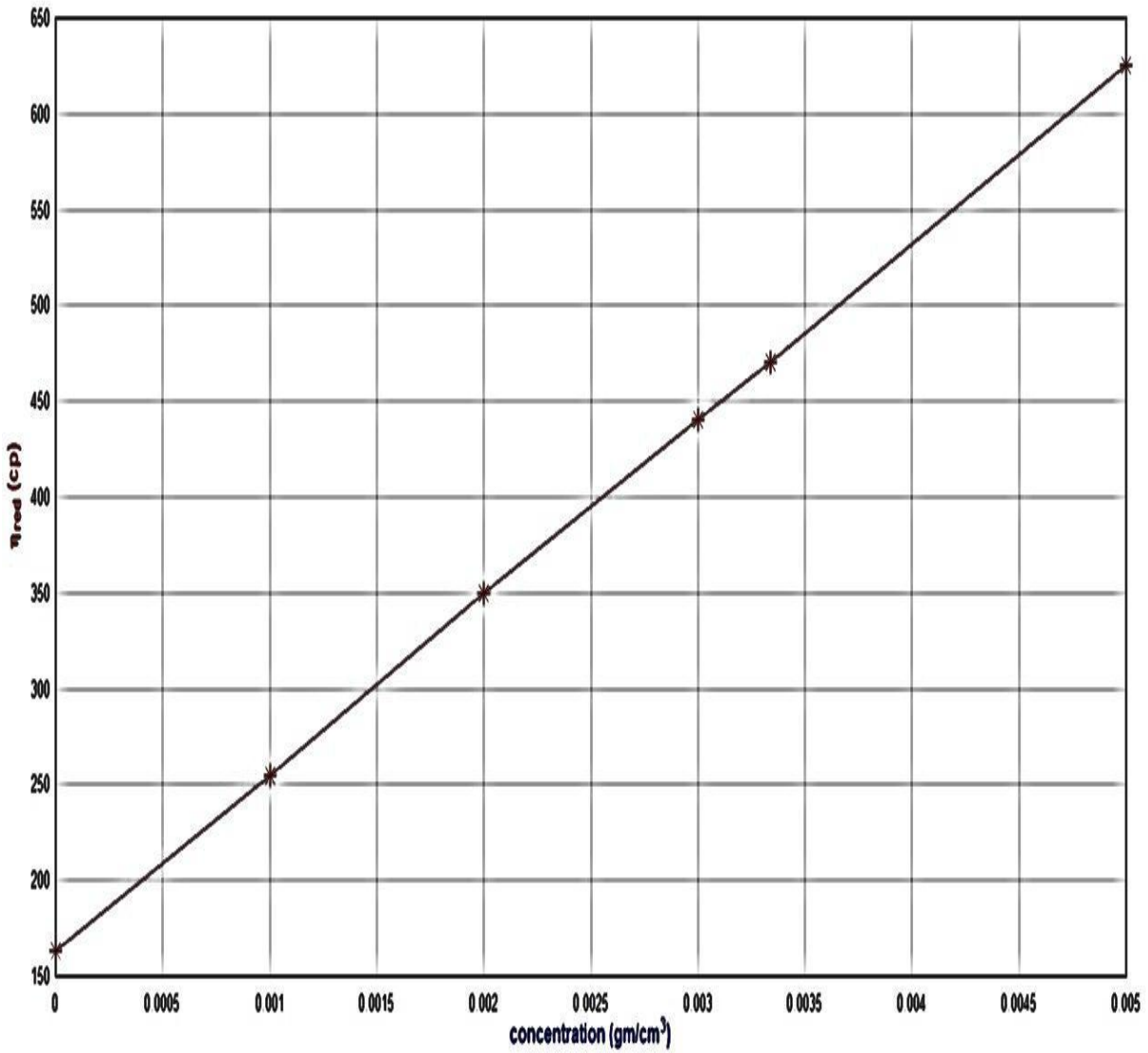


Figure 4.3: Relationship between concentration and reduction viscosity for CMC3.

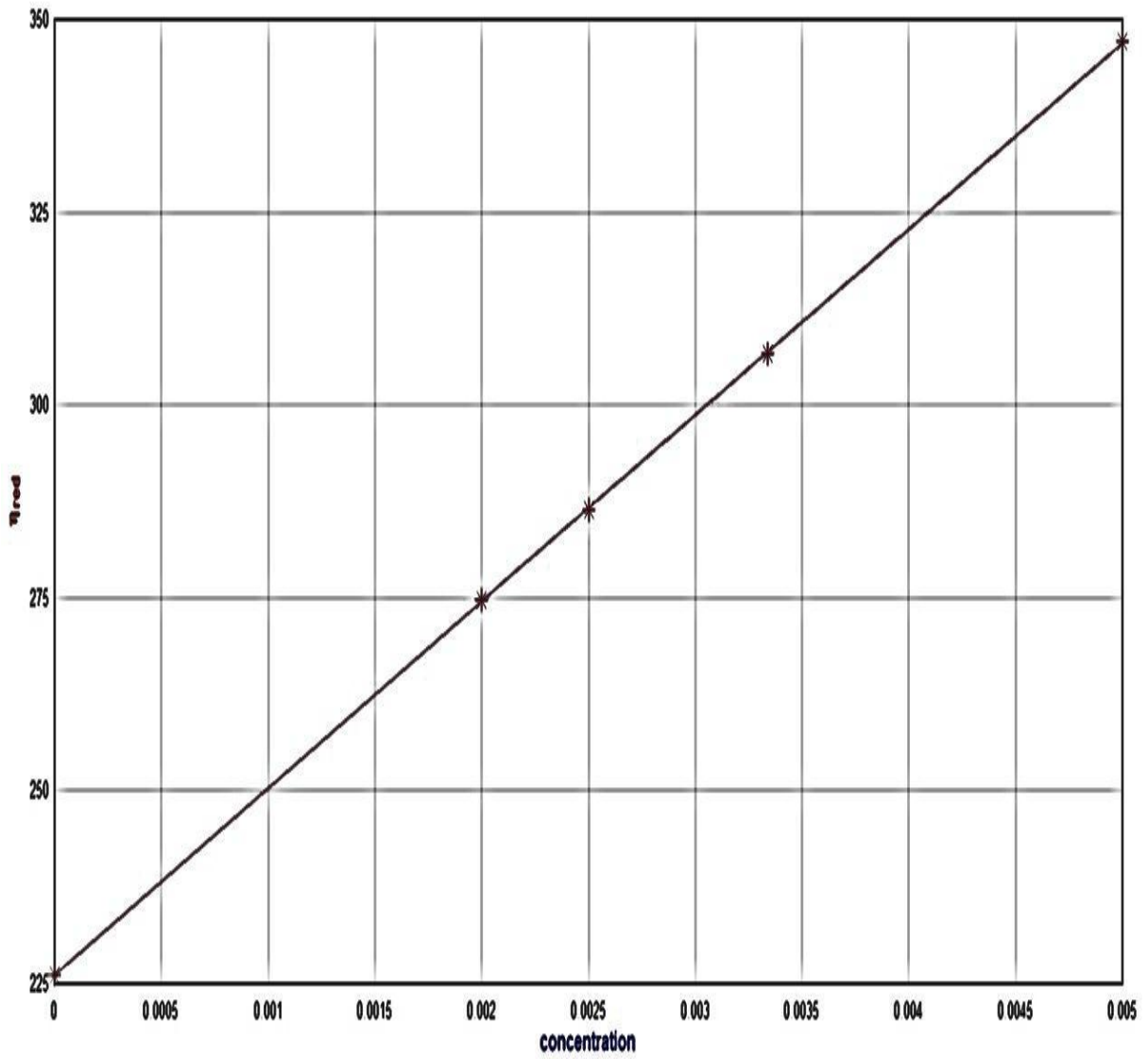


Figure 4.4: Relationship between concentration and reduction viscosity for CMC4.

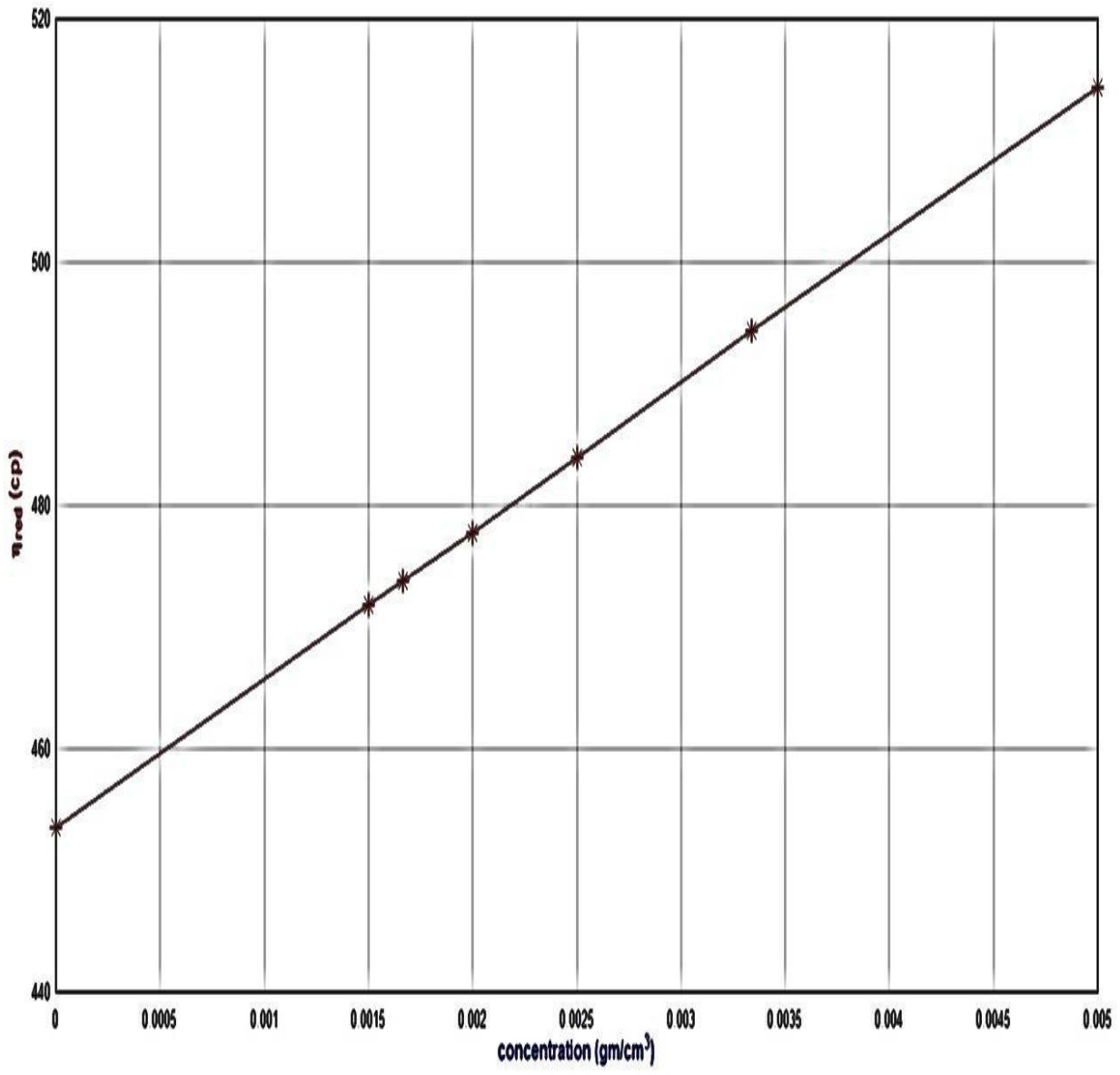


Figure 4.5: Relationship between concentration and reduction viscosity for CMC5.

These graphs represent an empirical equation by Huggins:

$$\eta_{sp}/C = [\eta] + K_H \times [\eta]^2 \times C \quad \dots (2.17)$$

The Huggins coefficient K_H depends on the solvent.

From Fig. 4.1 to 4.5, the slopes of the straight lines = $K_H \times [\eta]^2$ and the intercepts with the vertical axis represent the intrinsic viscosity $[\eta]$ as shown in table 4-1.

Table 4-1: Results of Huggins coefficient and intrinsic viscosity for five grades of Carboxymethyl cellulose.

samples	$[\eta]$ (cm ³ /gm)	$K_H \times [\eta]^2$	K_H
CMC1	67.549	5177.5	1.135
CMC2	150.62	6806.9	0.3
CMC3	163.55	92223	3.448
CMC4	226.09	24193	0.473
CMC5	453.56	12164	0.059

The average molecular weights for the five samples have been estimated by using the Mark-Houwink equation. This equation for CMC in 6% NaOH in water at 25°C is given as [Bochek Y. P., 2002]:

$$[\eta] = 7.3 \times 10^{-3} Mv^{0.93} \quad \dots (2.13)$$

And the results have been given in table 4-2.

Table 4-2: Results of intrinsic viscosity and molecular weight for five grades of Carboxymethyl cellulose.

CMC No.	Intrinsic viscosity (cm ³ /gm)	Molecular Weight Mv (gm/mol)
1	18,400	19,918
2	43,582	45,700
3	47,618	76,693
4	67,450	83,139
5	75,522	148,800

The results of flow time in capillary viscometer for five grades of CMC in different solution showed direct proportionality with the concentration, Π_{sp} and Π_{red} are also direct proportionality with flow time as noticed in their relationships (4.1 and 4.2) as obviously cleared in tables appendix B

The intrinsic viscosity values have been gotten from the interception at (C→0) from the definition of $[\eta]$ in equation (2.5), the values of $[\eta]$ in table (4-1) showed direct proportionality with Π_{sp} lead to increase $[\eta]$ with the increasing of flow time, the results of Huggins coefficient shown in table (4-1).

Because of unknown Mwt for CMC solutions so they have been estimated from the intrinsic viscosity measurements and from equation (4.5), the values of Mv from $(19 \times 10^3$ to 28×10^4 kg/kmol) as in table (4.2).

4.2 Measurement of dynamic viscometer with rotational viscometer for concentrated solution calculation:

At higher concentrations of polymer, a network structure is formed or not. In an ideal entanglement network, the average molecular weight between the adjacent points of entanglement (M_e) is a very important structure parameter which can be estimated through viscosity measurement where (M_e) can be deduced or not from plot of $\log \eta_0$ and $\log M$.

Where η_0 is the viscosity of the solution after extrapolation to $Y=0$. And RPM is revolution per minute.

The viscometer readings of seven grades for dynamic viscosity at different concentrations with different RPM(s) have been given in tables' appendix C.

The data of table C-1 appendix C have been plotted in Figs 4.6 to 4.10 for Conc.

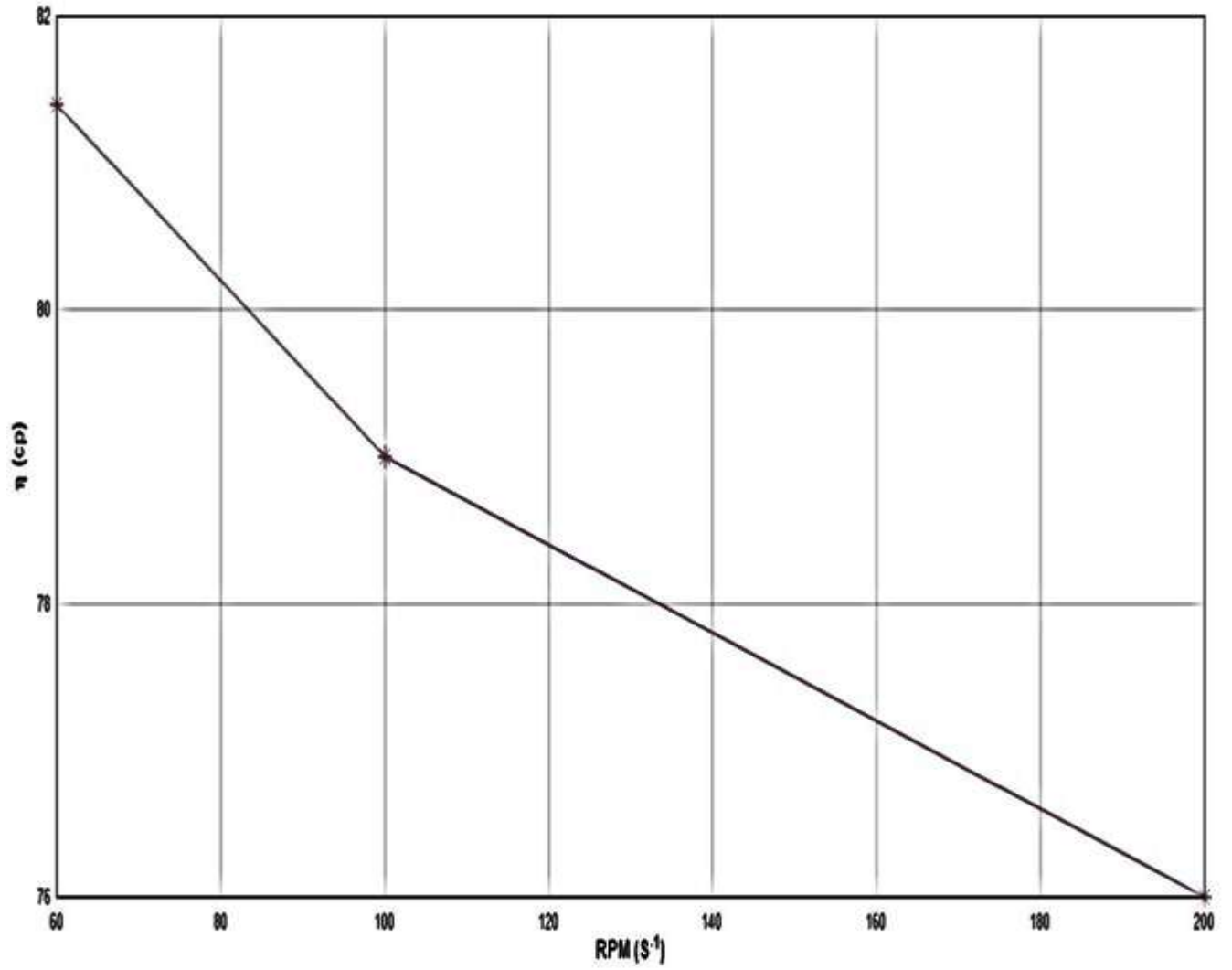


Figure 4.6: Relationship between η and RPM for CMC1 for conc. 1%

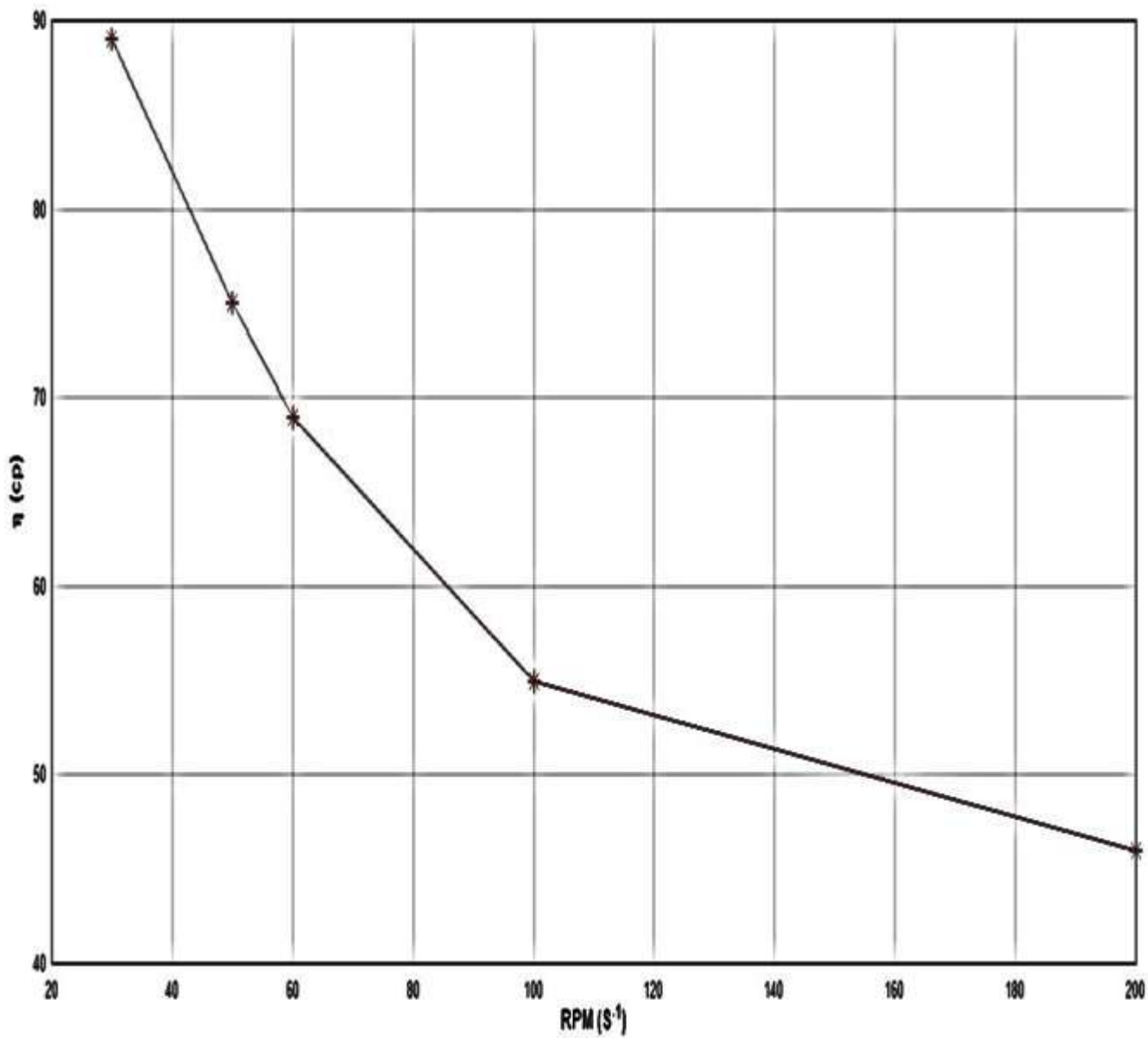


Figure 4.7: Relationship between η and RPM for CMC2 for Conc. 1%.

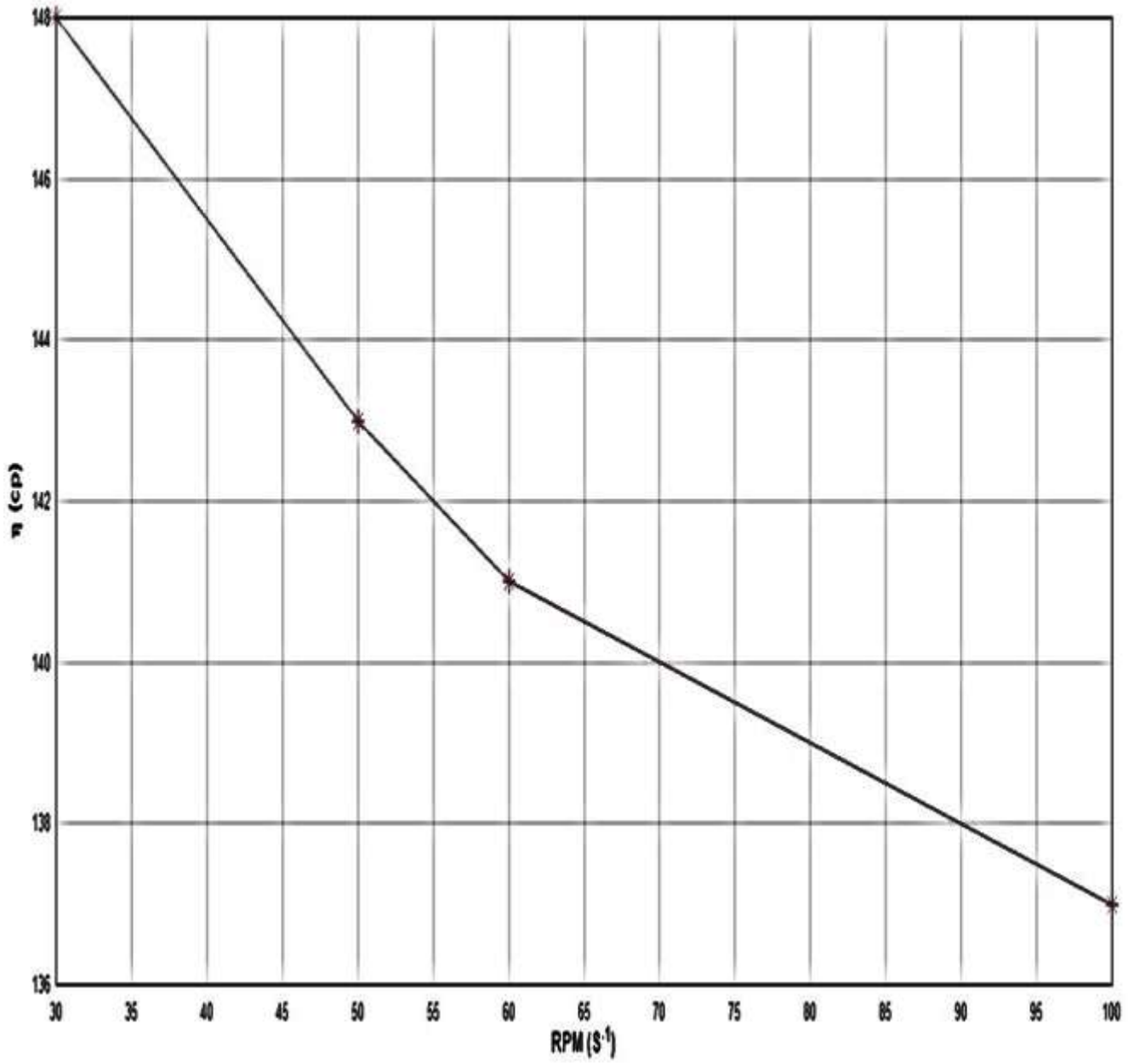


Figure 4.8: Relationship between η and RPM for CMC3 for Conc. 1%.

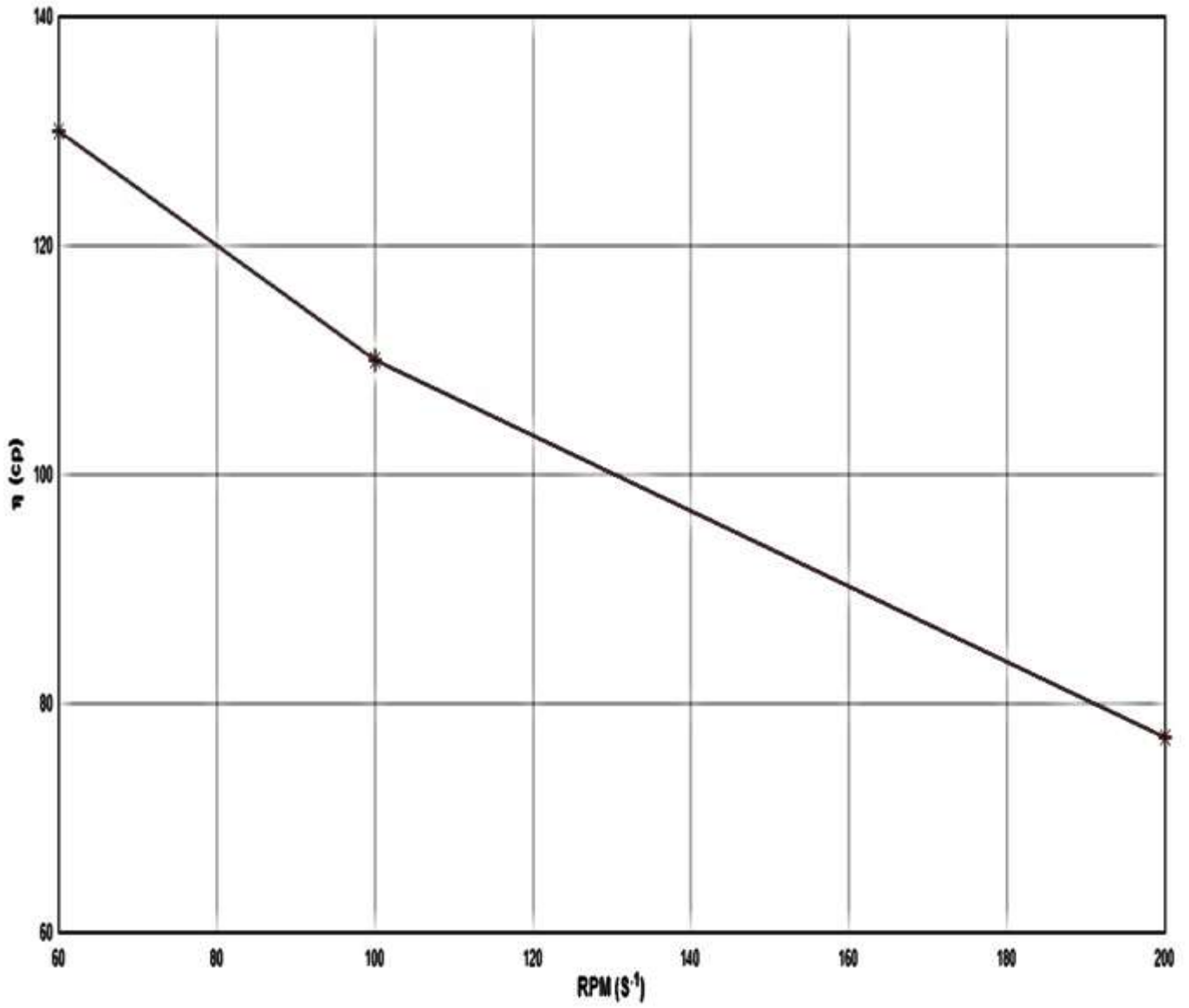


Figure 4.9: Relationship between η and RPM for CMC4 for Conc. 1%.

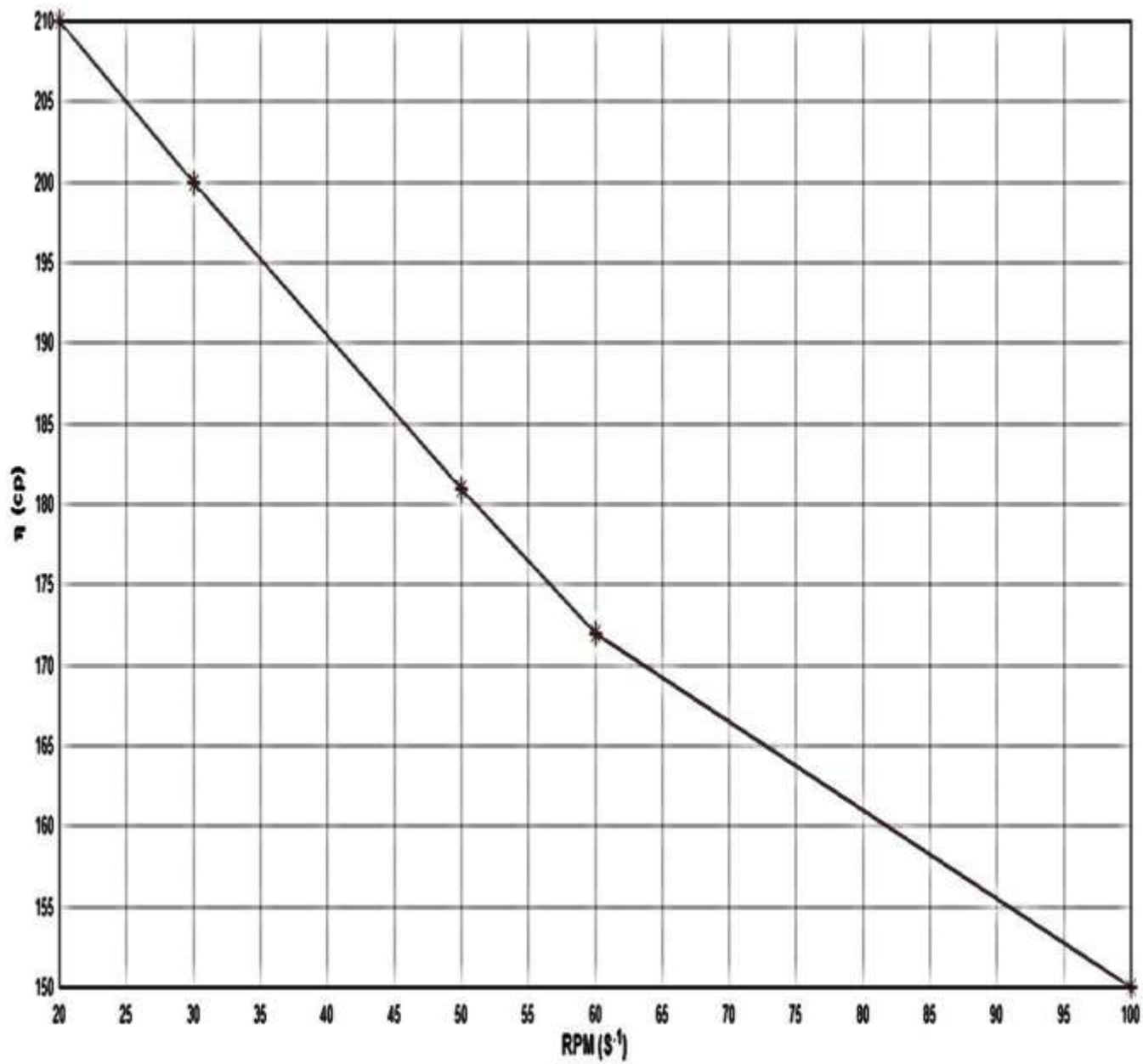


Figure 4.10: Relationship between η and RPM for CMC5 for Conc. 1%.

The data of table C-2 appendix C have been plotted in Figs 4.11 to 4.15 for conc. 2%.

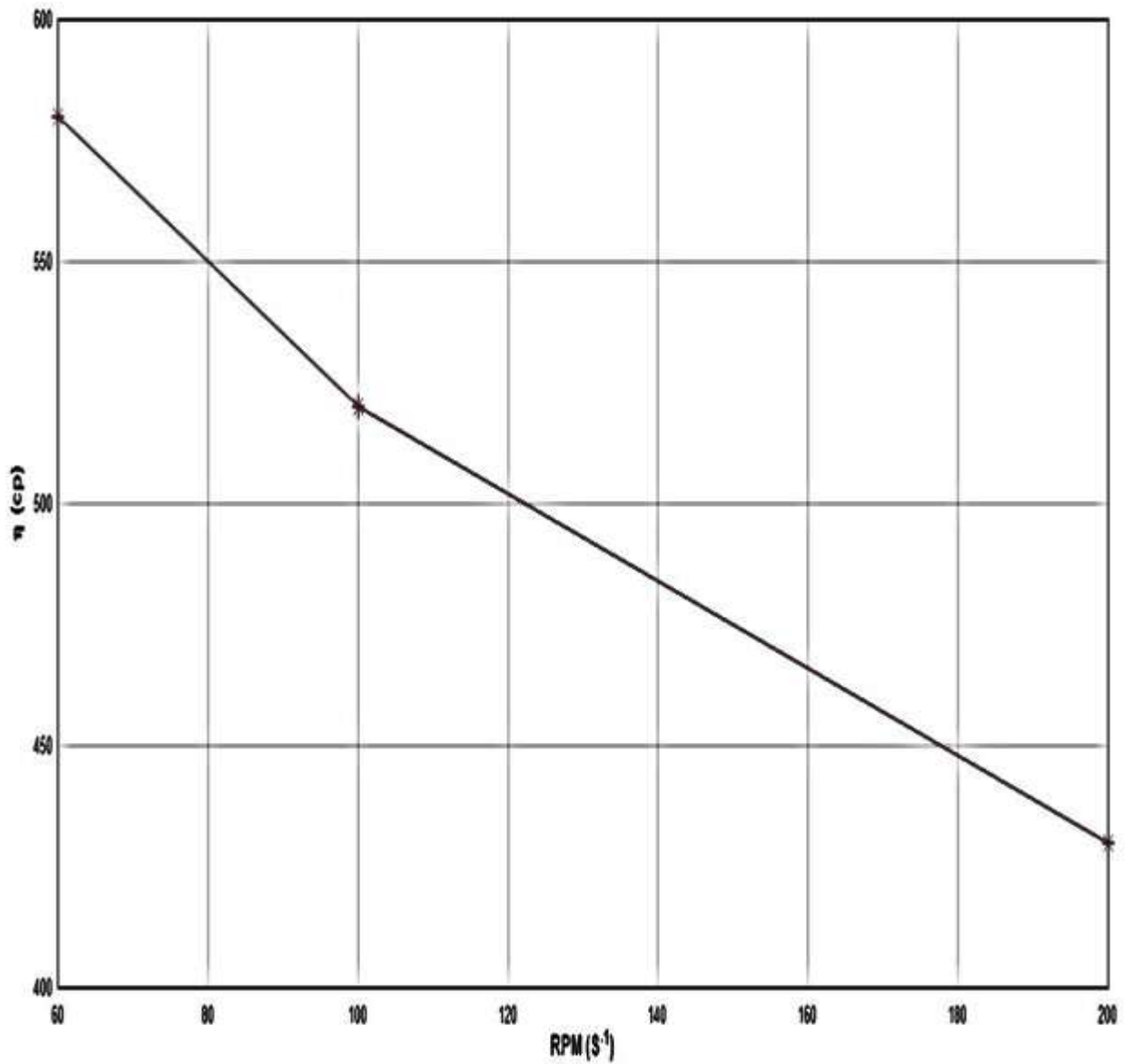


Figure 4.11: Relationship between η and RPM for CMC1 for Conc. 2%.

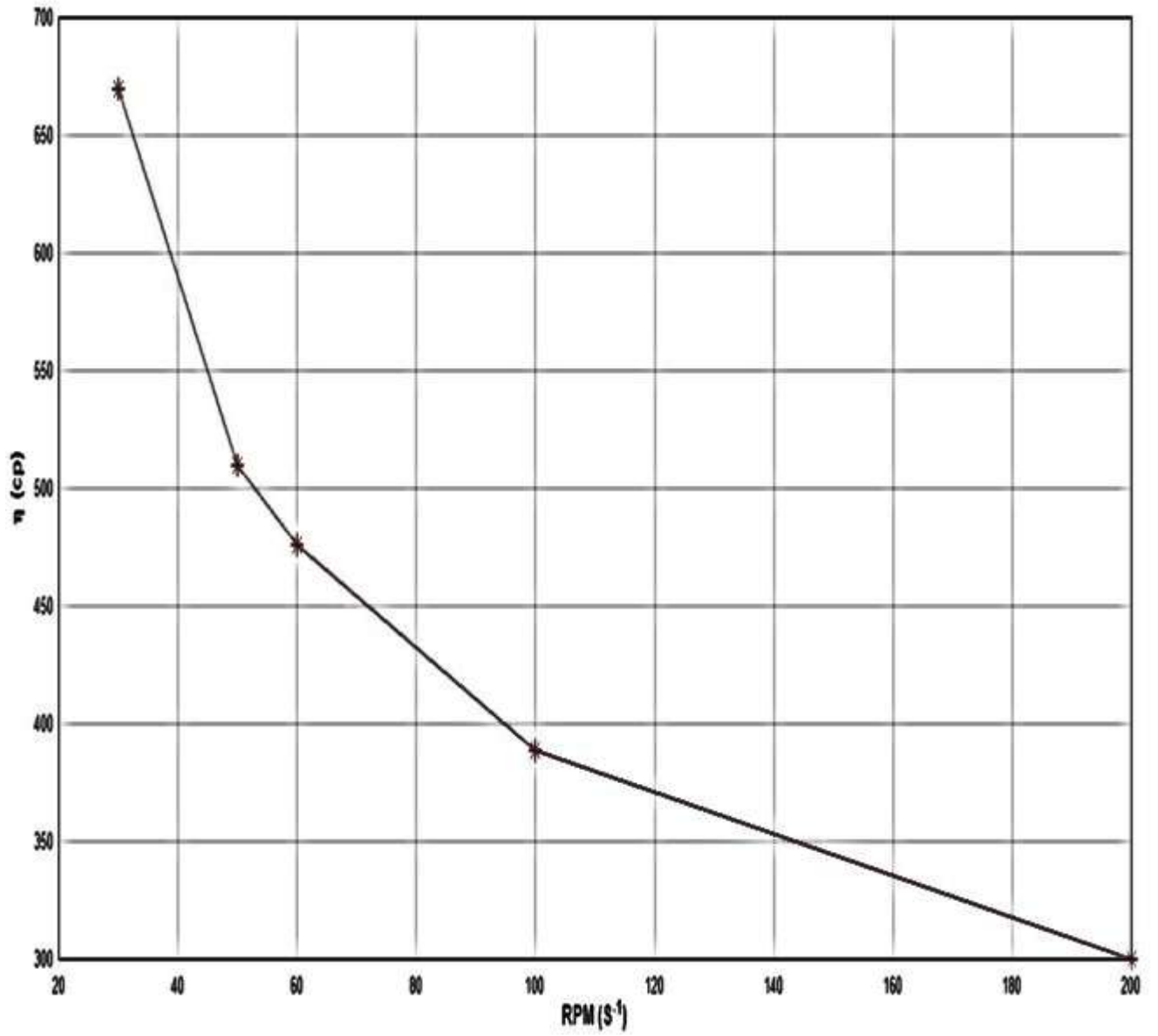


Figure 4.12: Relationship between η and RPM for CMC2 for Conc. 2%.

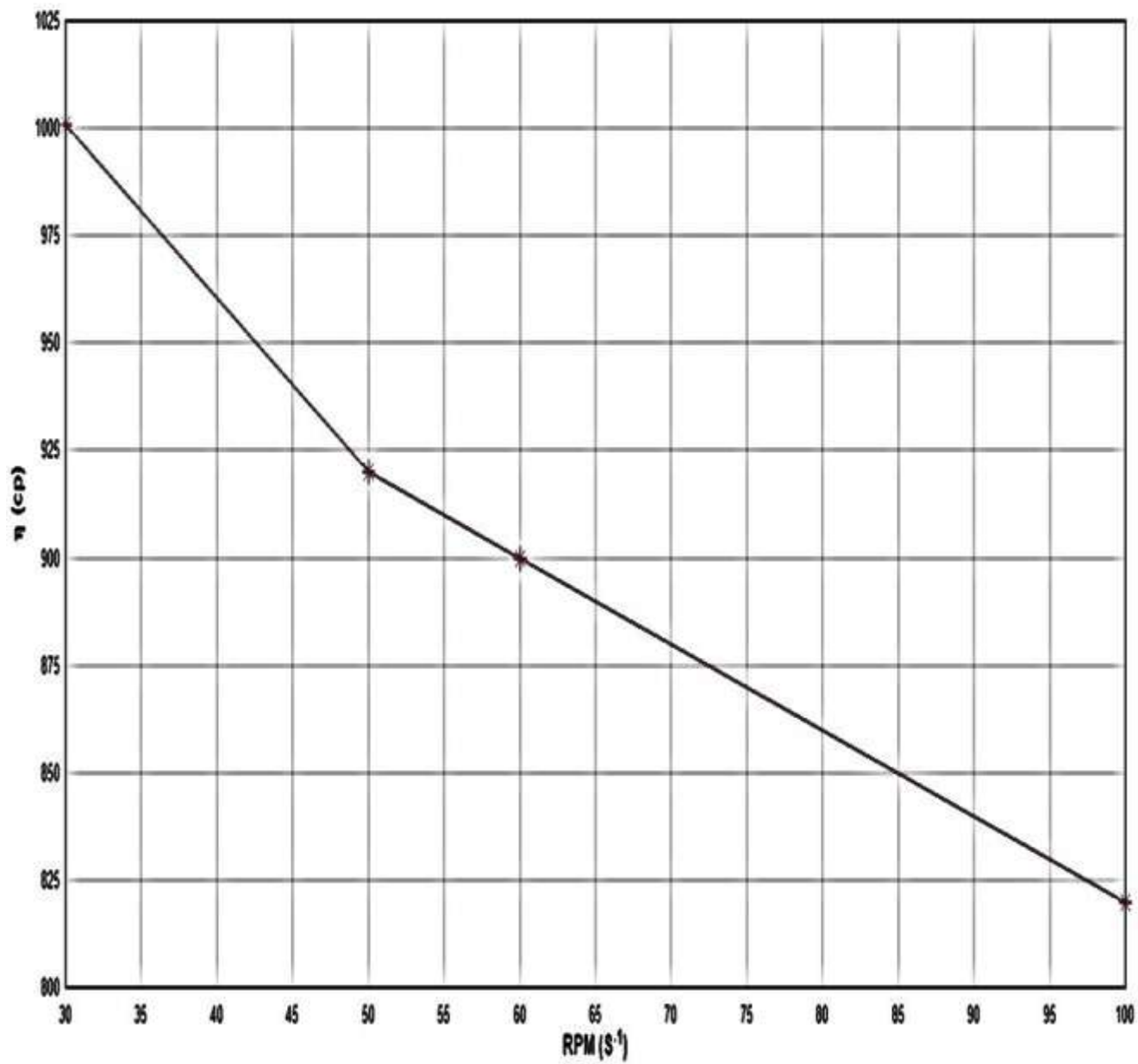


Figure 4.13: Relationship between η and RPM for CMC3 for Conc. 2%.

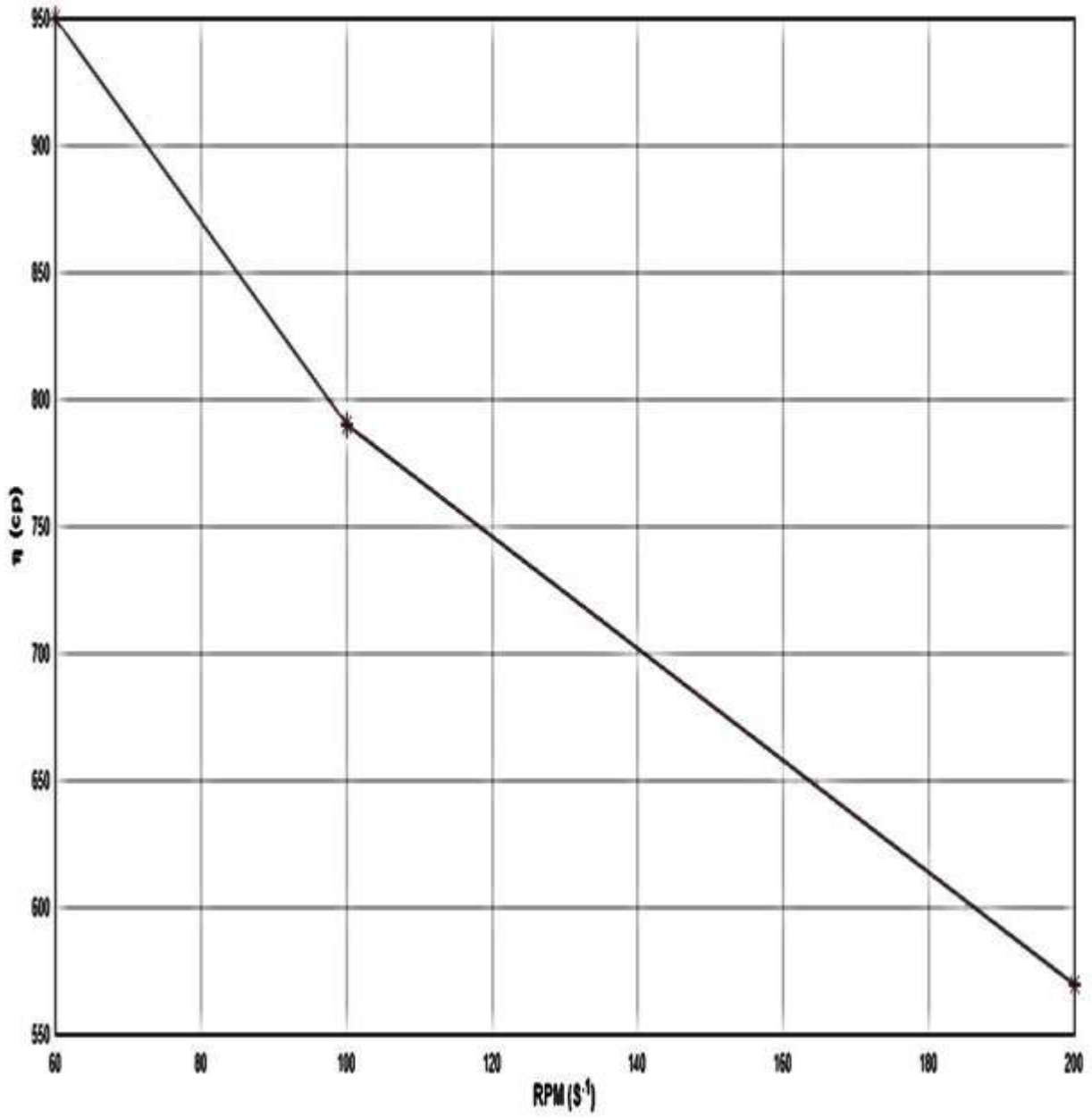


Figure 4.14: Relationship between η and RPM for CMC4 for Conc. 2%.

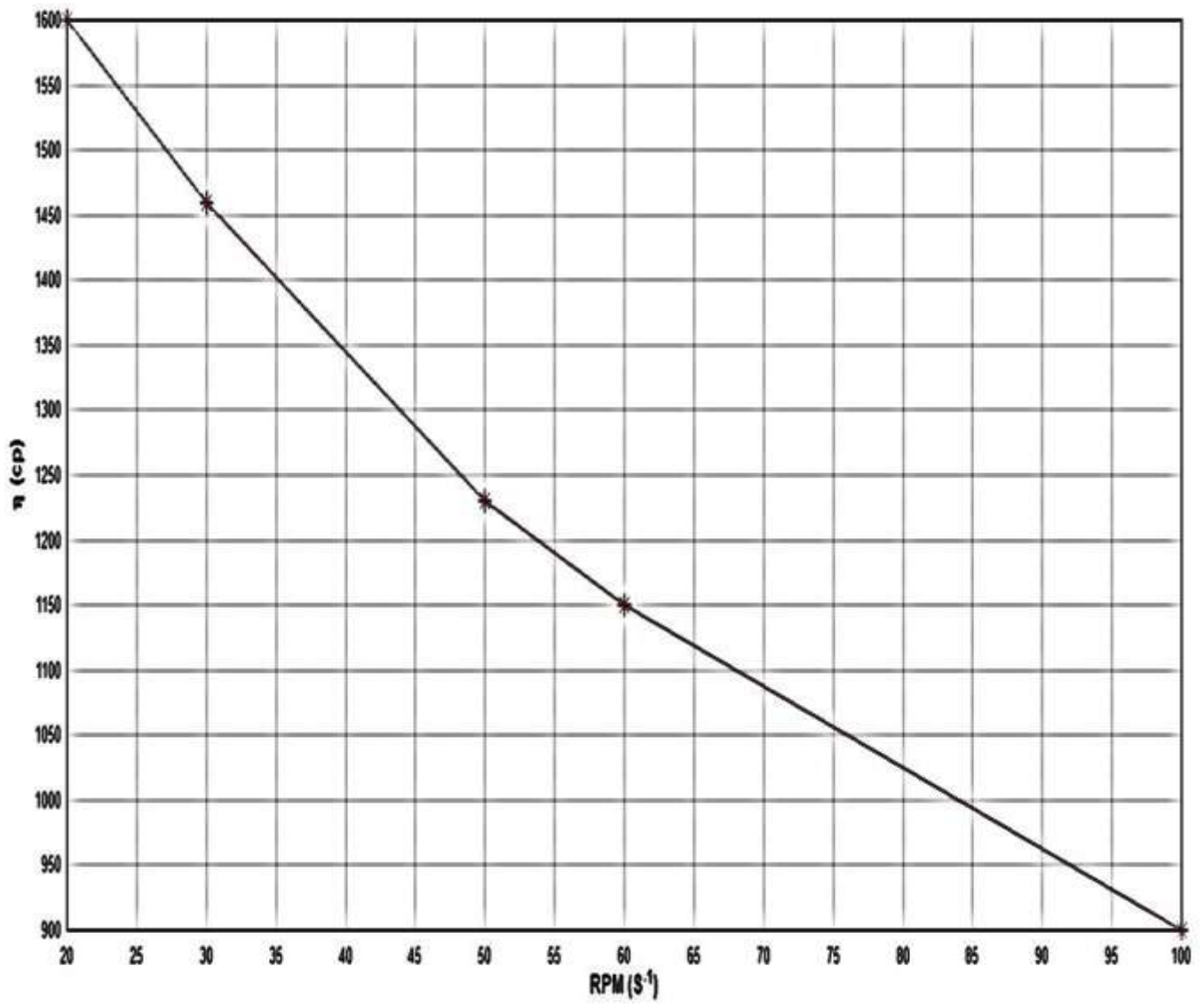


Figure 4.15: Relationship between η and RPM for CMC5 for Conc. 2%.

The data of table C-3 appendix C have been plotted in Figs 4.16 to 4.20 for Conc. 3%

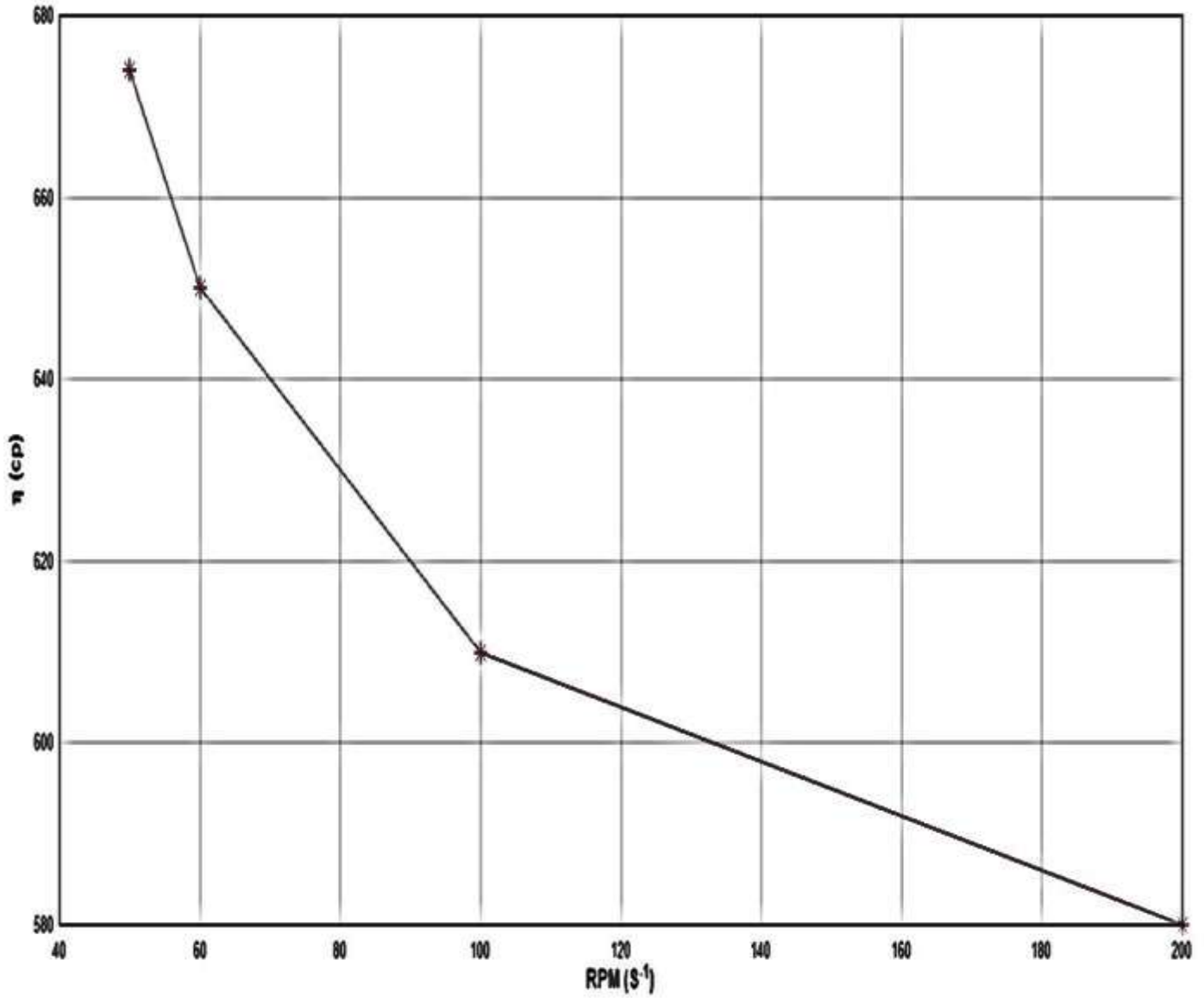


Figure 4.16: Relationship between η and RPM for CMC1 for Conc. 3%.

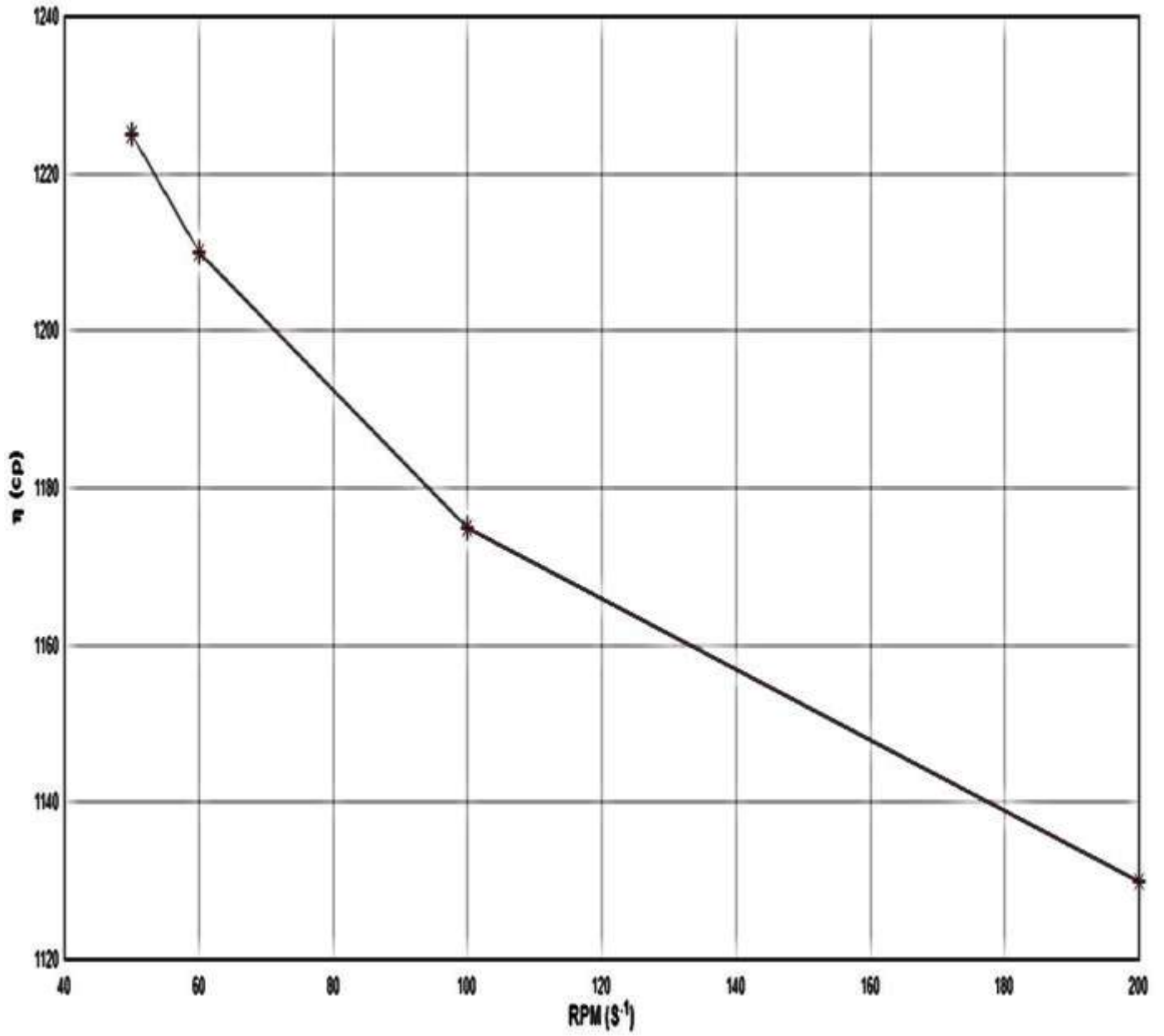


Figure 4.17: Relationship between η and RPM for CMC2 for Conc. 3%.

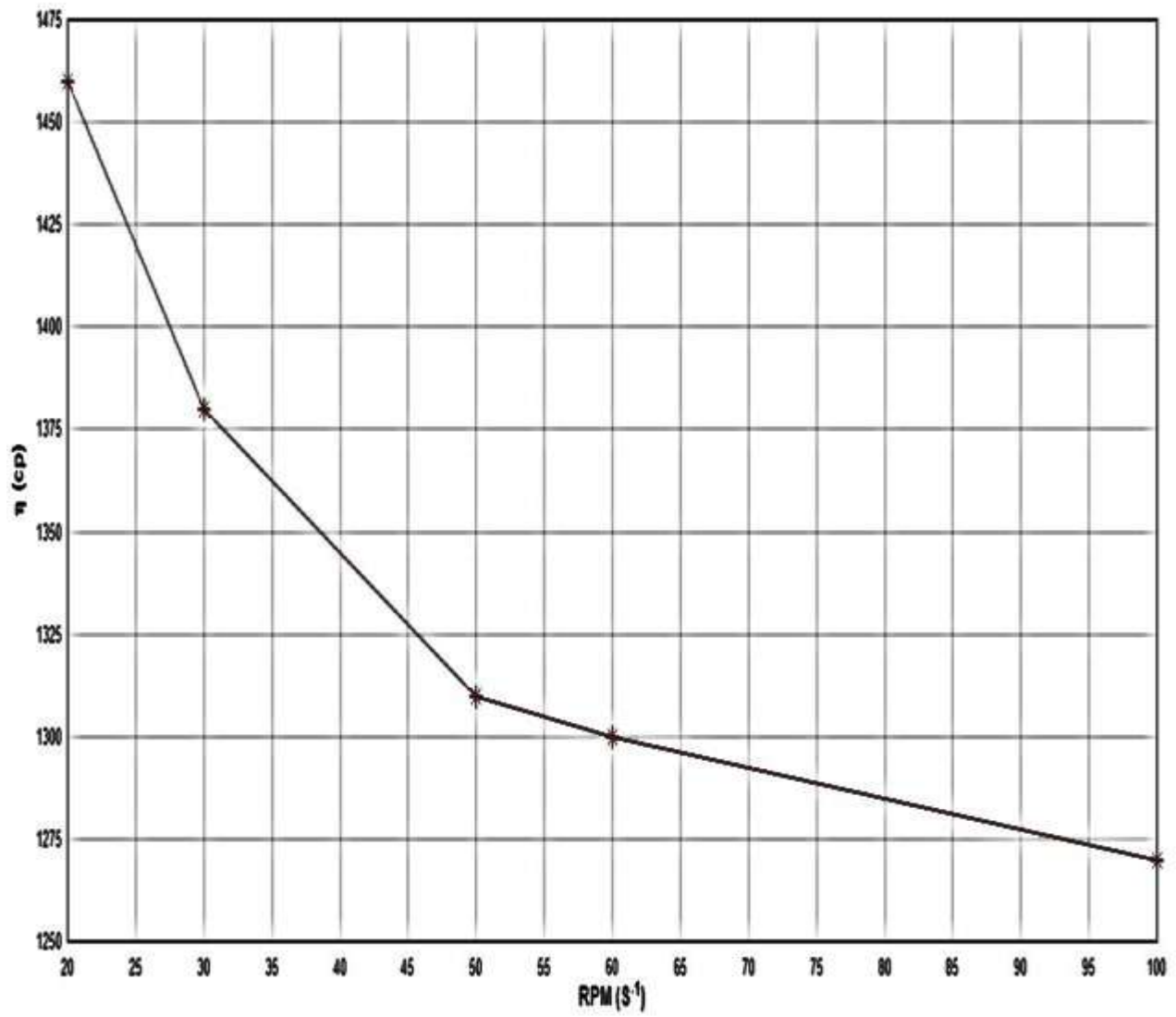


Figure 4.18: Relationship between η and RPM for CMC3 for Conc. 3%.

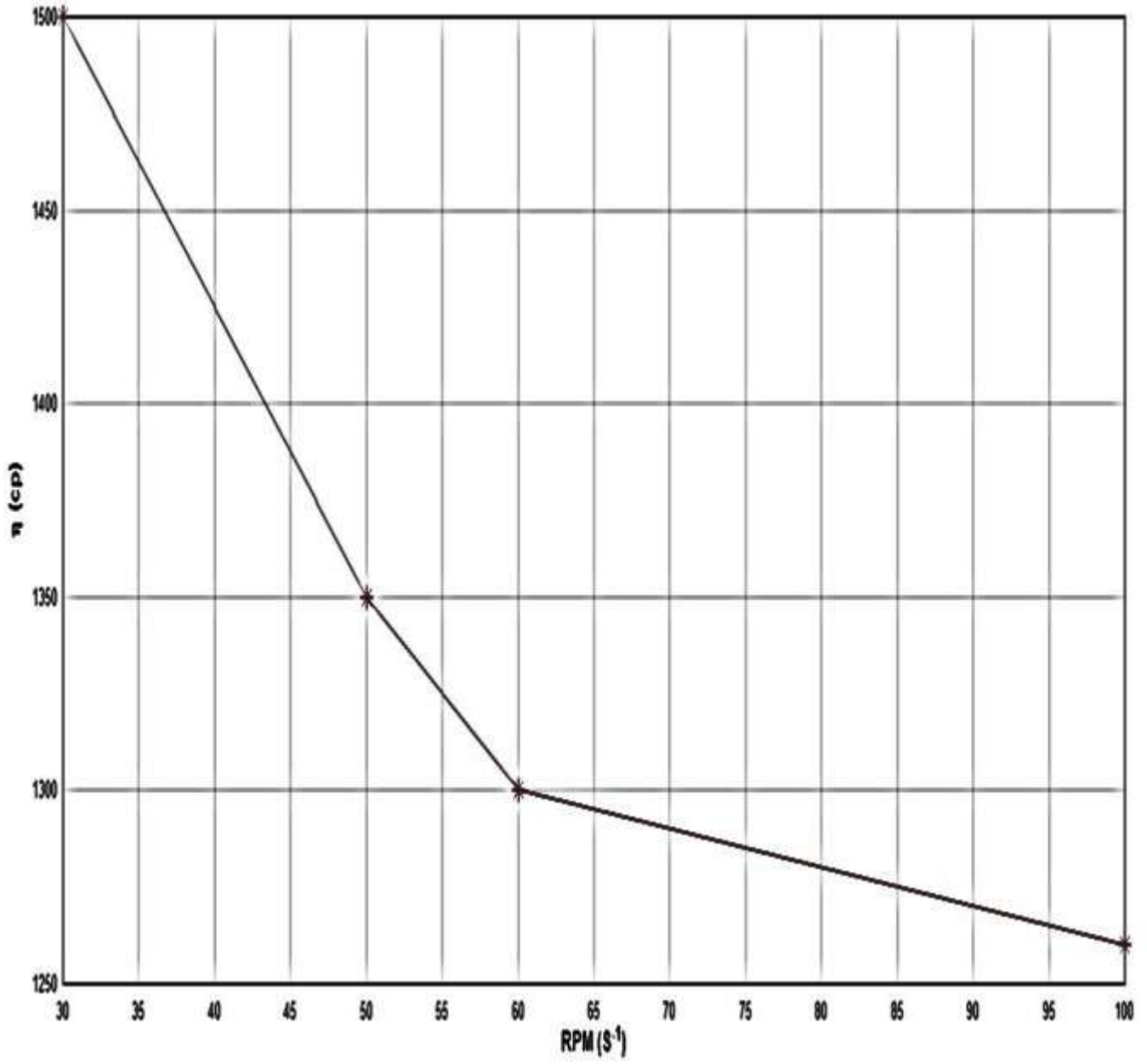


Figure 4.19: Relationship between η and RPM for CMC4 for Conc. 3%.

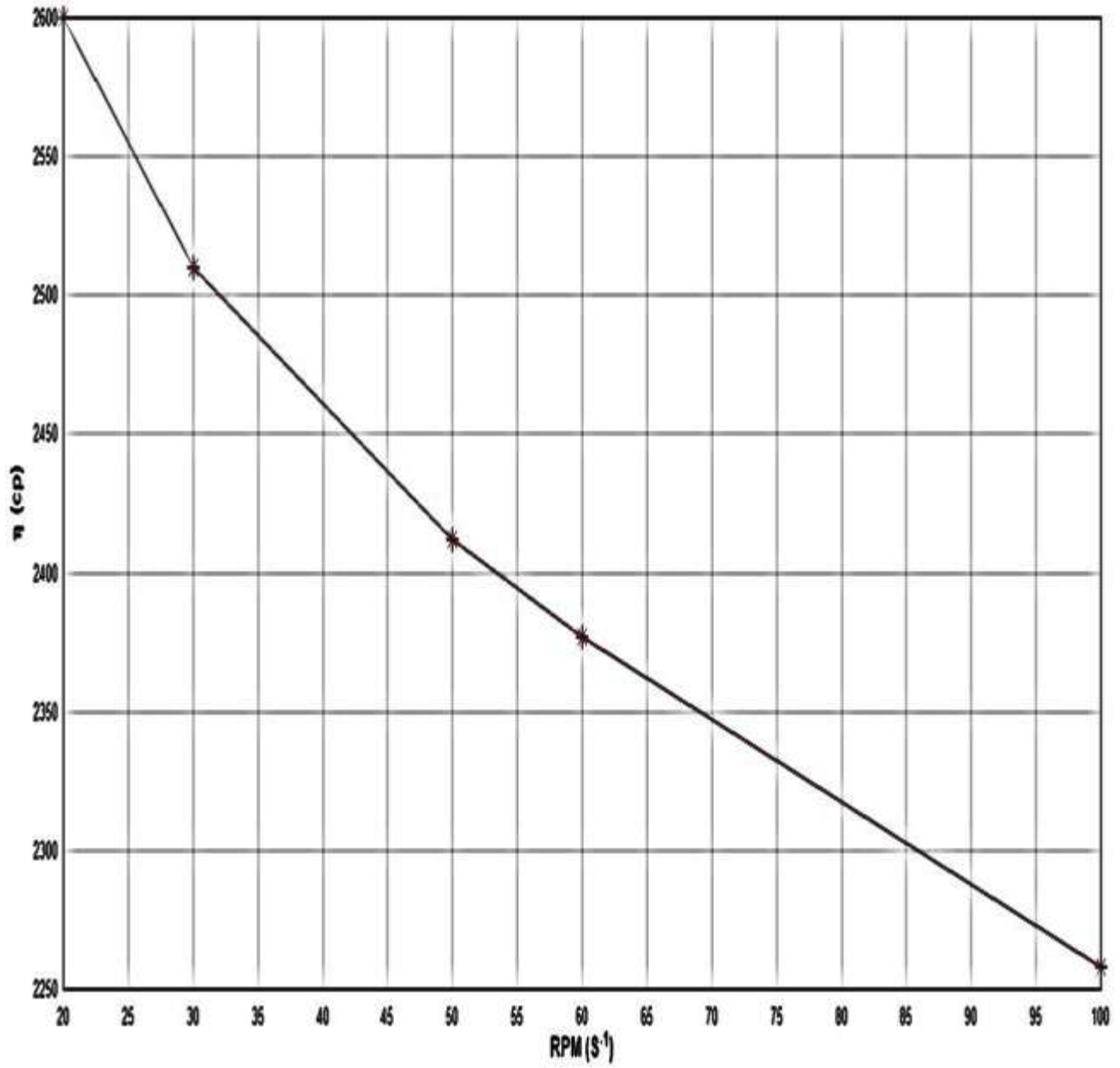


Figure 4.20: Relationship between η and RPM for CMC5 for Conc. 3%.

The data of table C-4 appendix C have been plotted in Figs 4.21 to 4.25 for Conc. 4%.

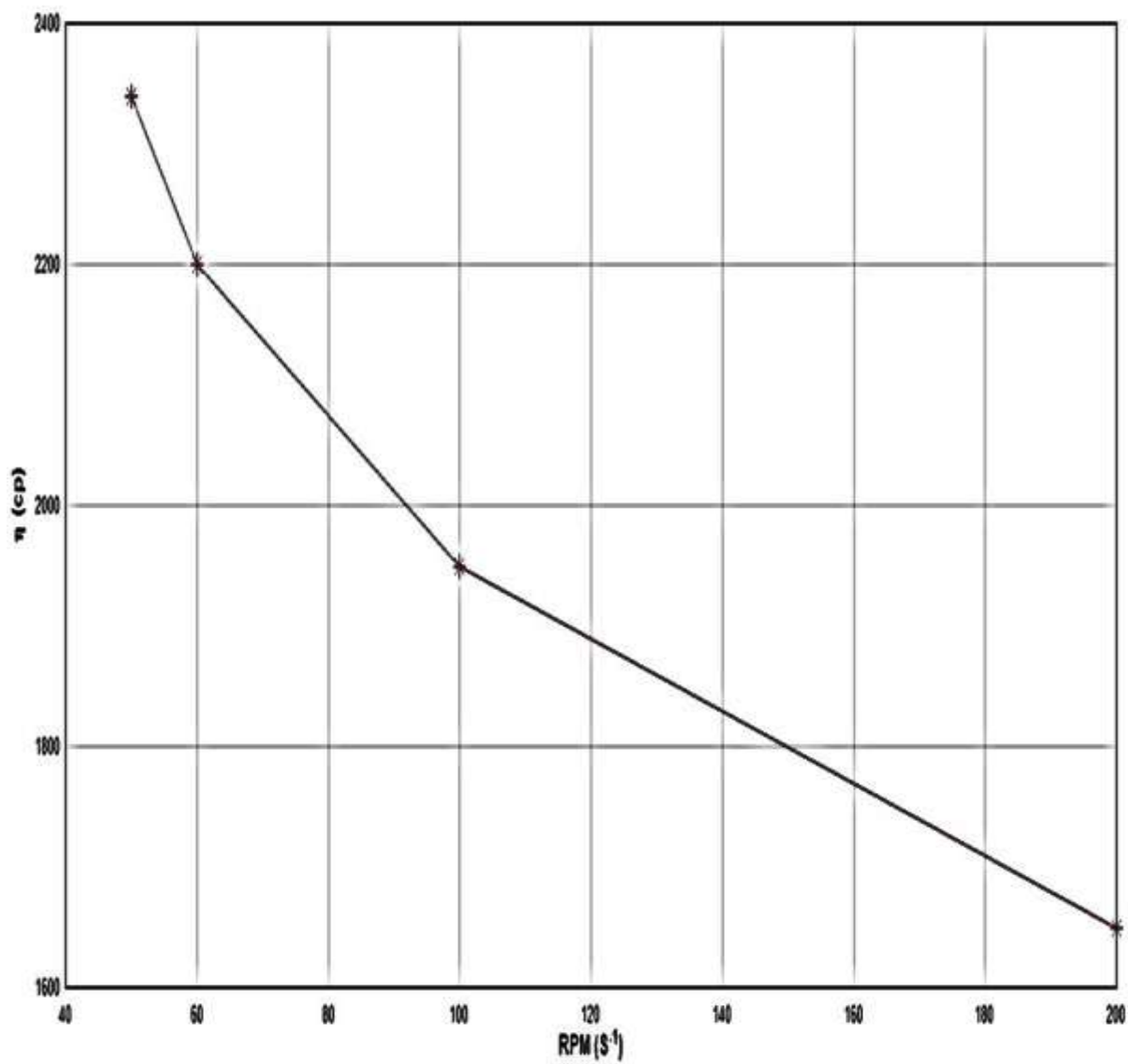


Figure 4.21: Relationship between η and RPM for CMC1 for Conc. 4%.

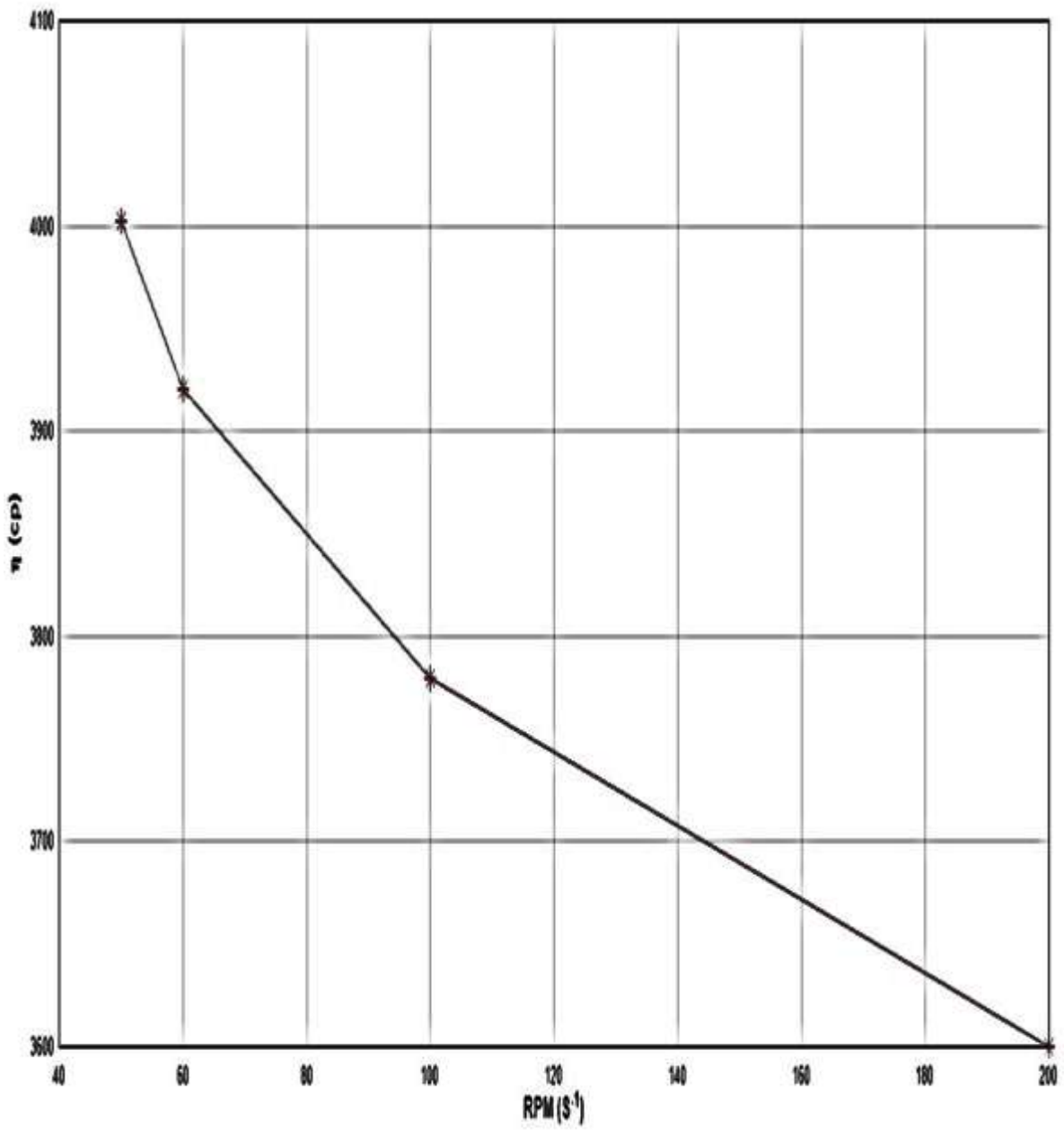


Figure 4.22: Relationship between η and RPM for CMC2 for Conc. 4%.

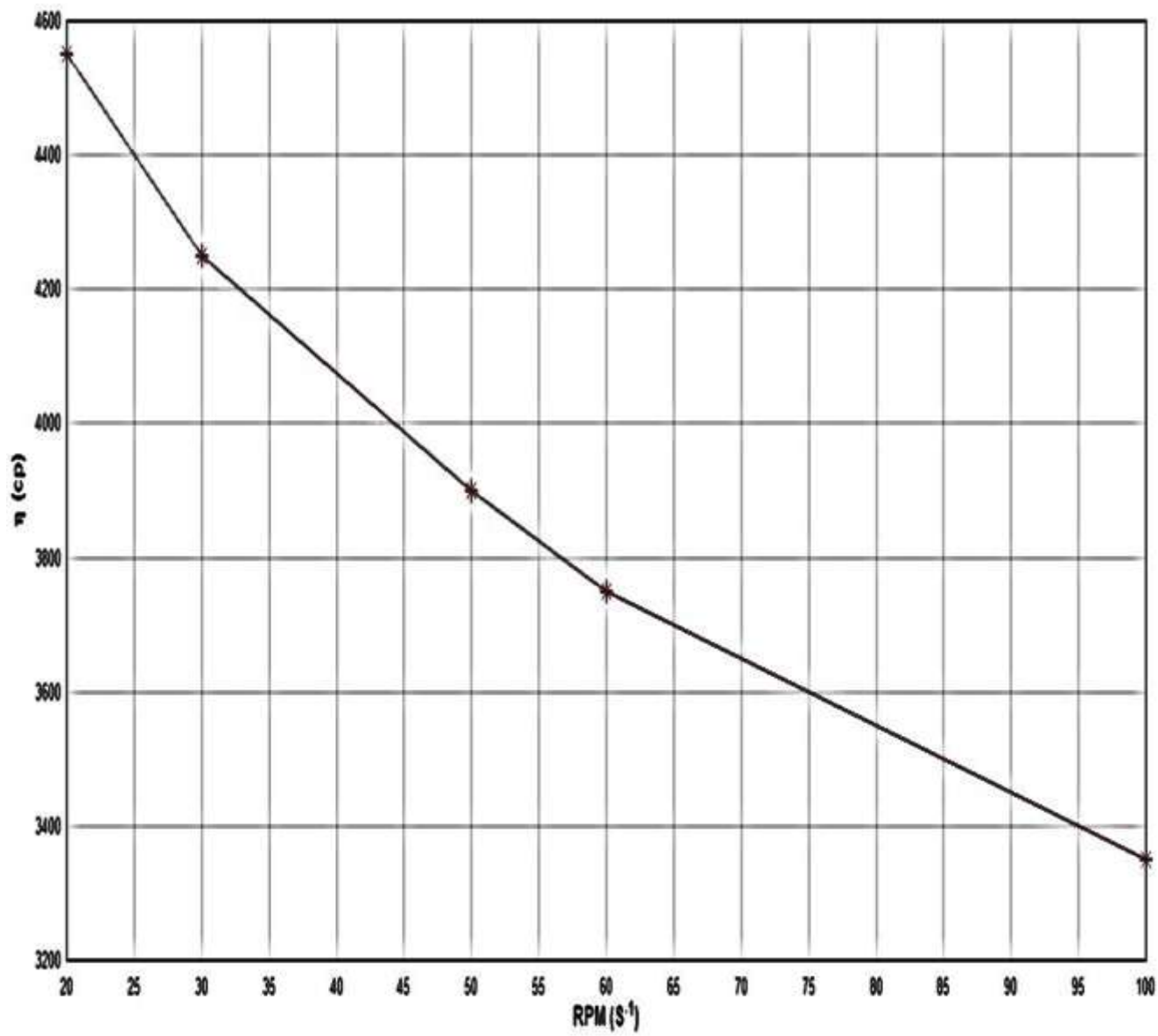


Figure 4.23: Relationship between η and RPM for CMC3 for Conc. 4%.

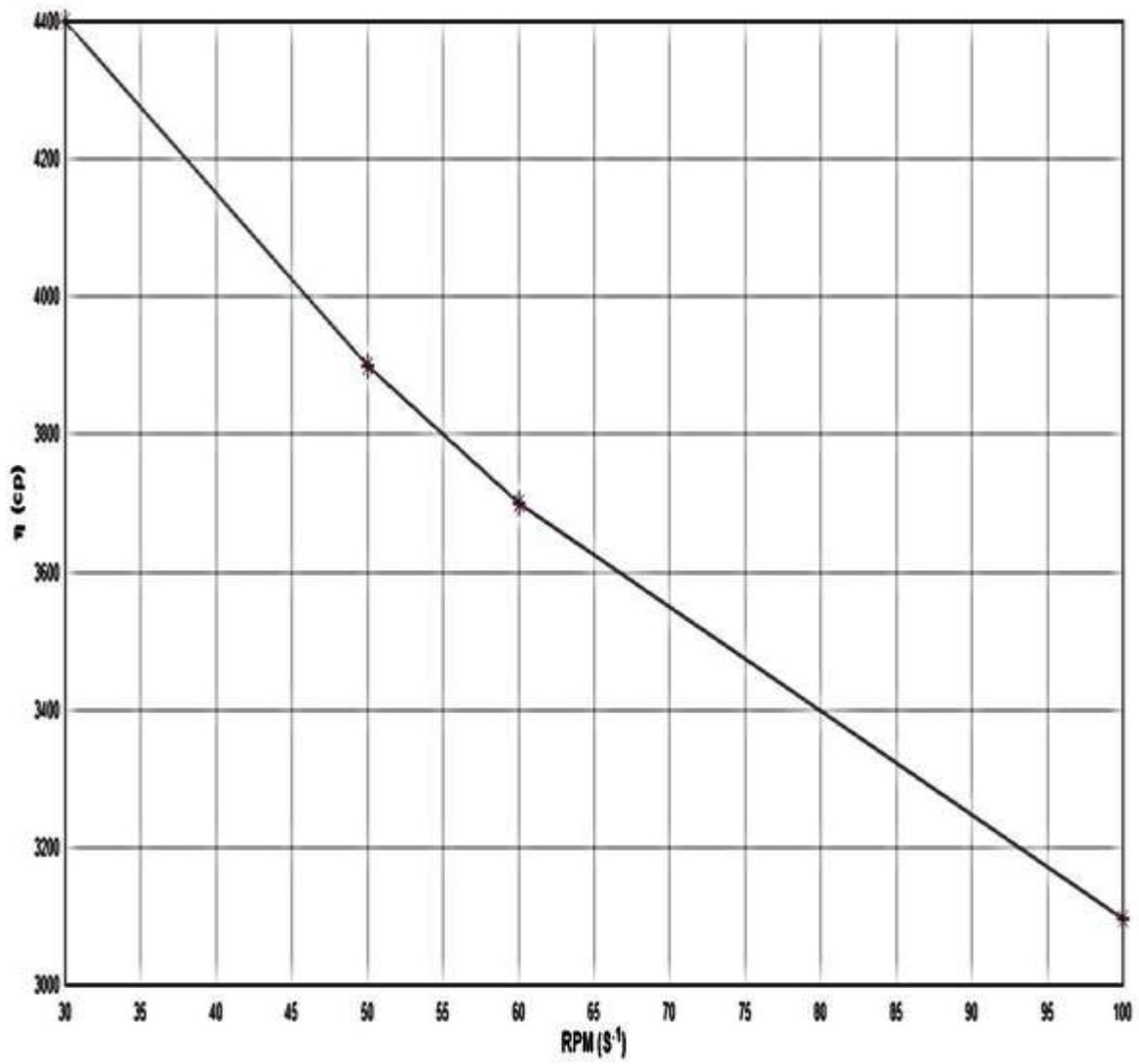


Figure 4.24: Relationship between η and RPM for CMC4 for Conc. 4%.

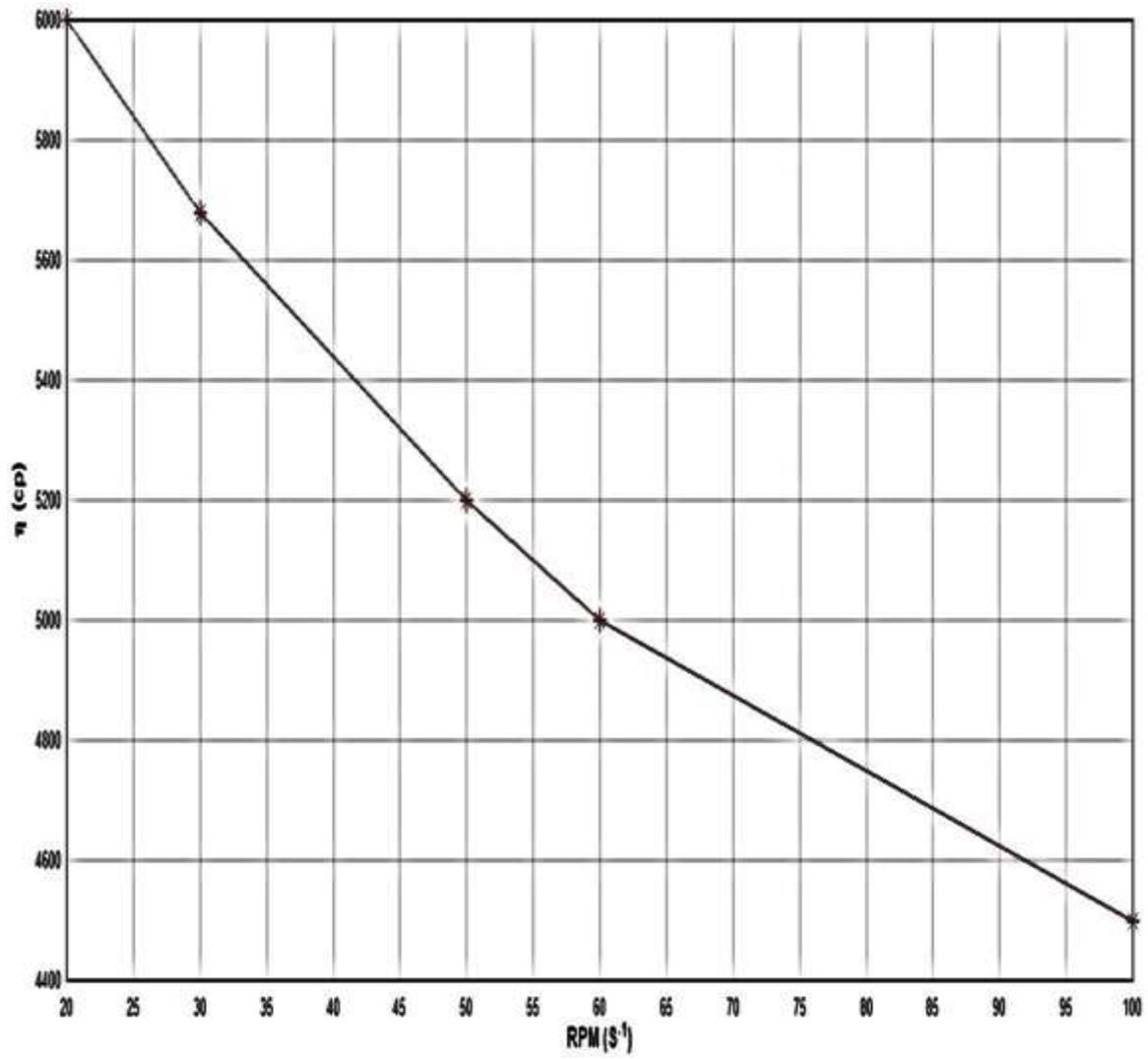


Figure 4.25: Relationship between η and RPM for CMC5 for Conc. 4%.

The η_0 values have been gotten from power law calculations at RPM =0 as given below for each grade at different concentrations.

$$\eta = \eta_0 \left(\frac{RPM}{RPM_0}\right)^{n-1} \quad \dots(4.3)$$

Table 4-3 : the results of power law calculation for concentration 1%

CMC	η_0	η	n-1
1	83.231	102.74	-0.0569
2	109.68	299.45	-0.358
3	151.25	184.04	-0.0644
4	155.1	933.35	-0.4691
5	221.55	402.35	-0.2096

Table 4-4 : the results of power law calculation for concentration 2%

CMC	η_0	η	n-1
1	645.4228	1625.4	-0.25
2	828.5018	2661.7	-0.416
3	1061.675	1755.2	-0.165
4	1078.459	5524.4	-0.427
5	1743.292	4789.2	-0.355

Table 4-5 : the results of power law calculation for concentration 3%

CMC	η_o	η	n-1
1	680.5656	1006.8	-0.106
2	1303.892	1534.3	-0.058
3	1434.256	1869.6	-0.087
4	1386.07	2423.1	-0.146
5	2637.41	3369	-0.086

Table 4-6 : the results of power law calculation for concentration 4%

CMC	η_o	η	n-1
1	2445.945	6114.4	-0.248
2	4324.294	5337	-0.075
3	4541.382	8053	-0.188
4	3945.181	12057	-0.292
5	6232.857	10375	-0.179

Table 4-7: η_o and Mv of each CMC sample with all Conc.

CMC No.	η_o (cp) of Con. 1%	η_o (cp) of Conc. 2%	η_o (cp) of Conc. 3%	η_o (cp) of Conc. 4%	Mv. (gm/cm ³)
1	83.231	645.4228	680.5656	2445.945	18,400.71
2	109.68	828.5018	1303.892	4324.294	43,582.45
3	151.25	1061.675	1434.256	4541.382	47,618.06
4	155.1	1078.459	1386.07	3945.181	67,450.88
5	221.55	1743.292	2637.41	6232.857	142,593.20

The data in table 4-7 have been plotted log-log in the following graphs (4.26 to 4.29), each graph for each concentratins.

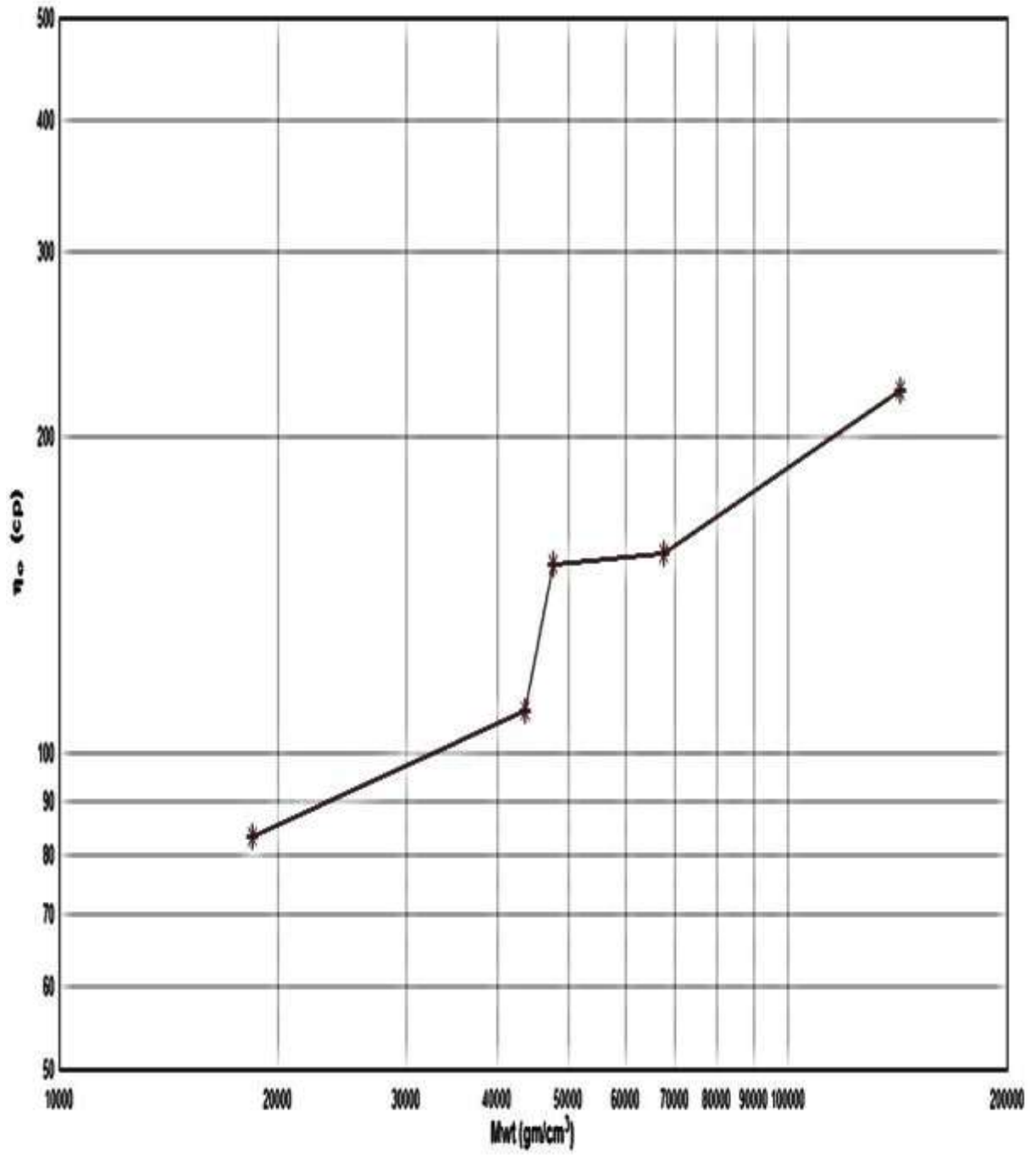


Figure 4.26: Relationship between $\log \bar{\eta}_0$ and $\log M_v$. for Conc. 1%.

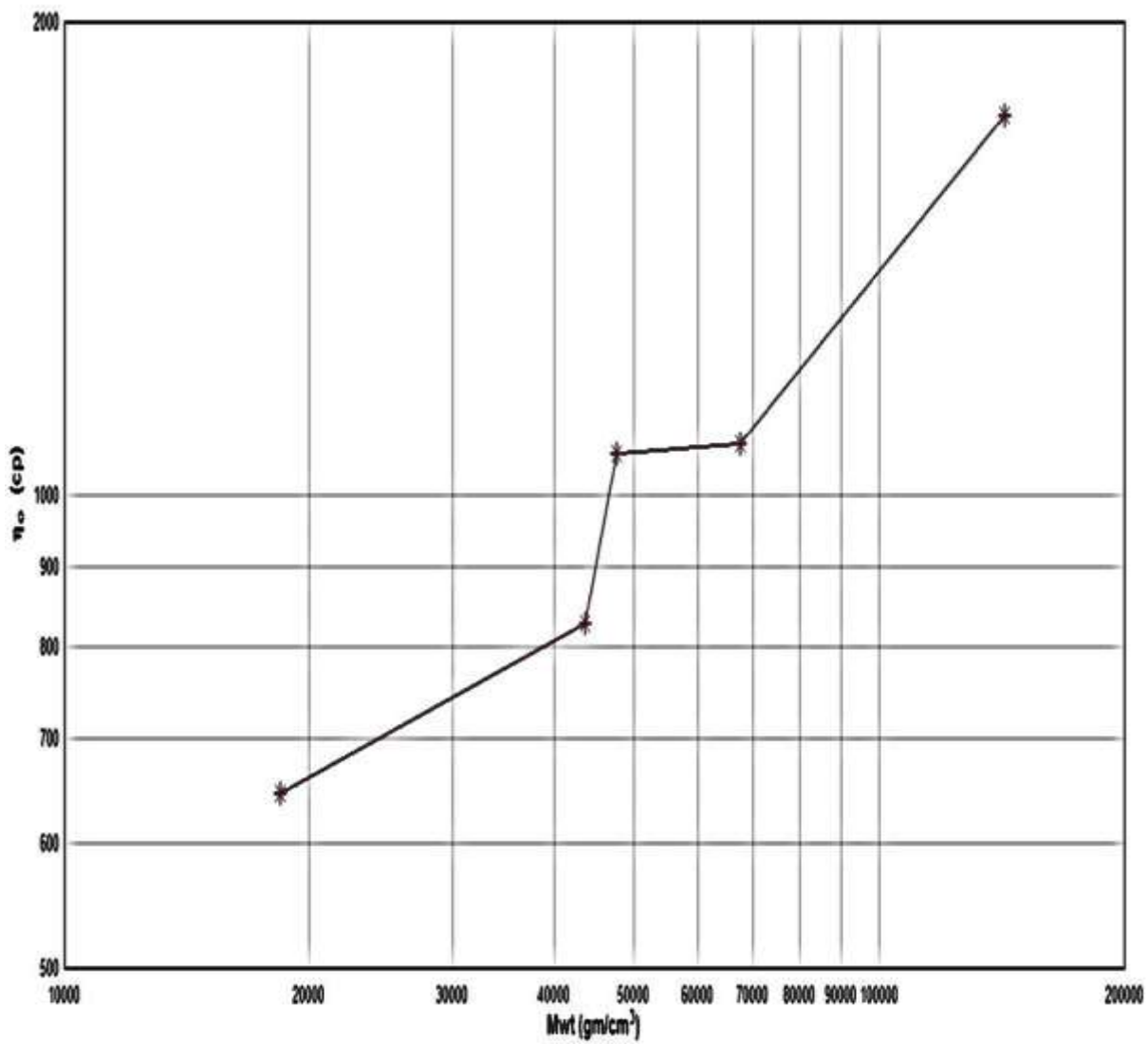


Figure 4.27: Relationship between $\log \eta_0$ and $\log M_w$ for Conc. 2%.

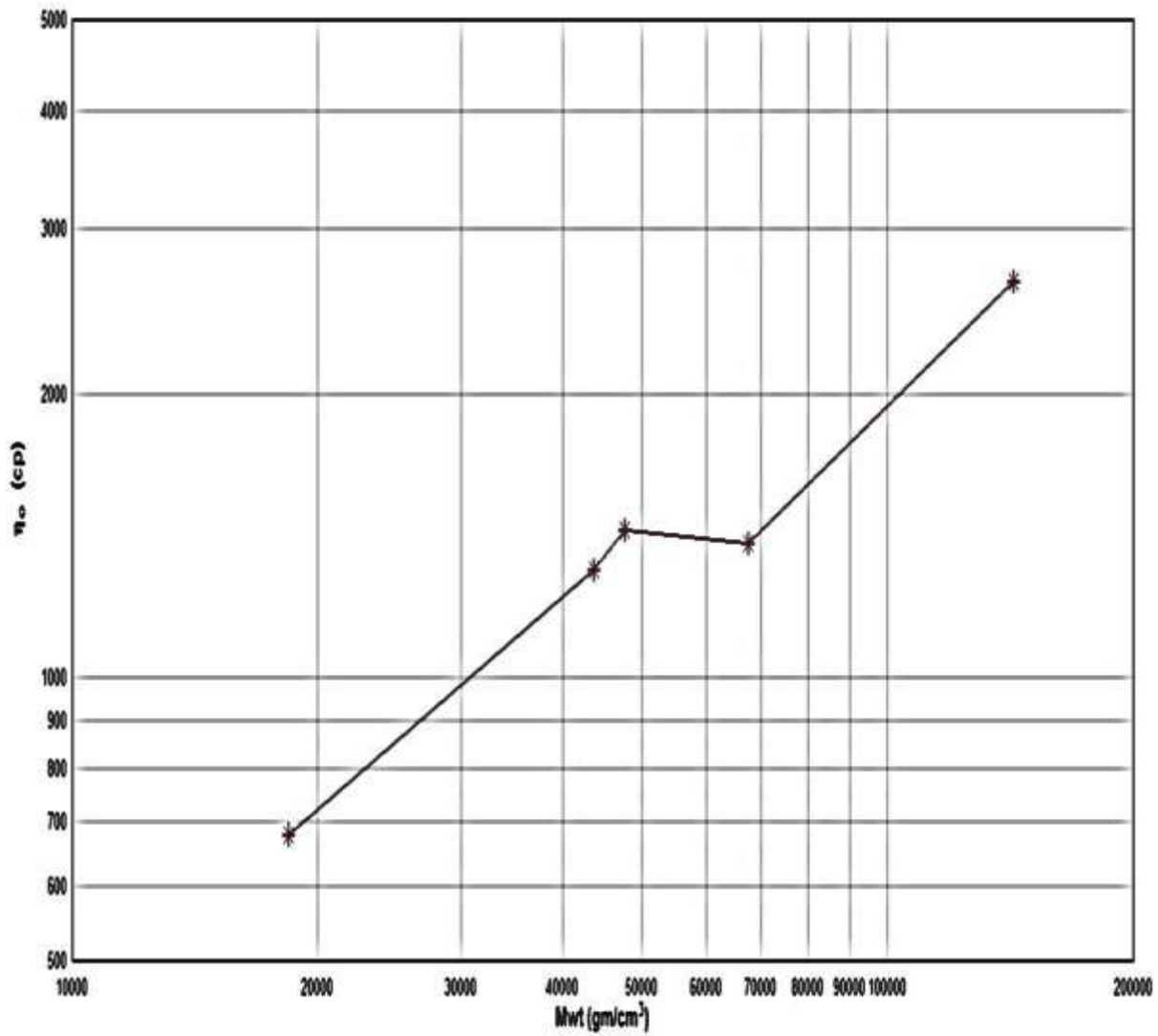


Figure 4.28: Relationship between $\log \eta_0$ and $\log M_v$. for Conc. 3%

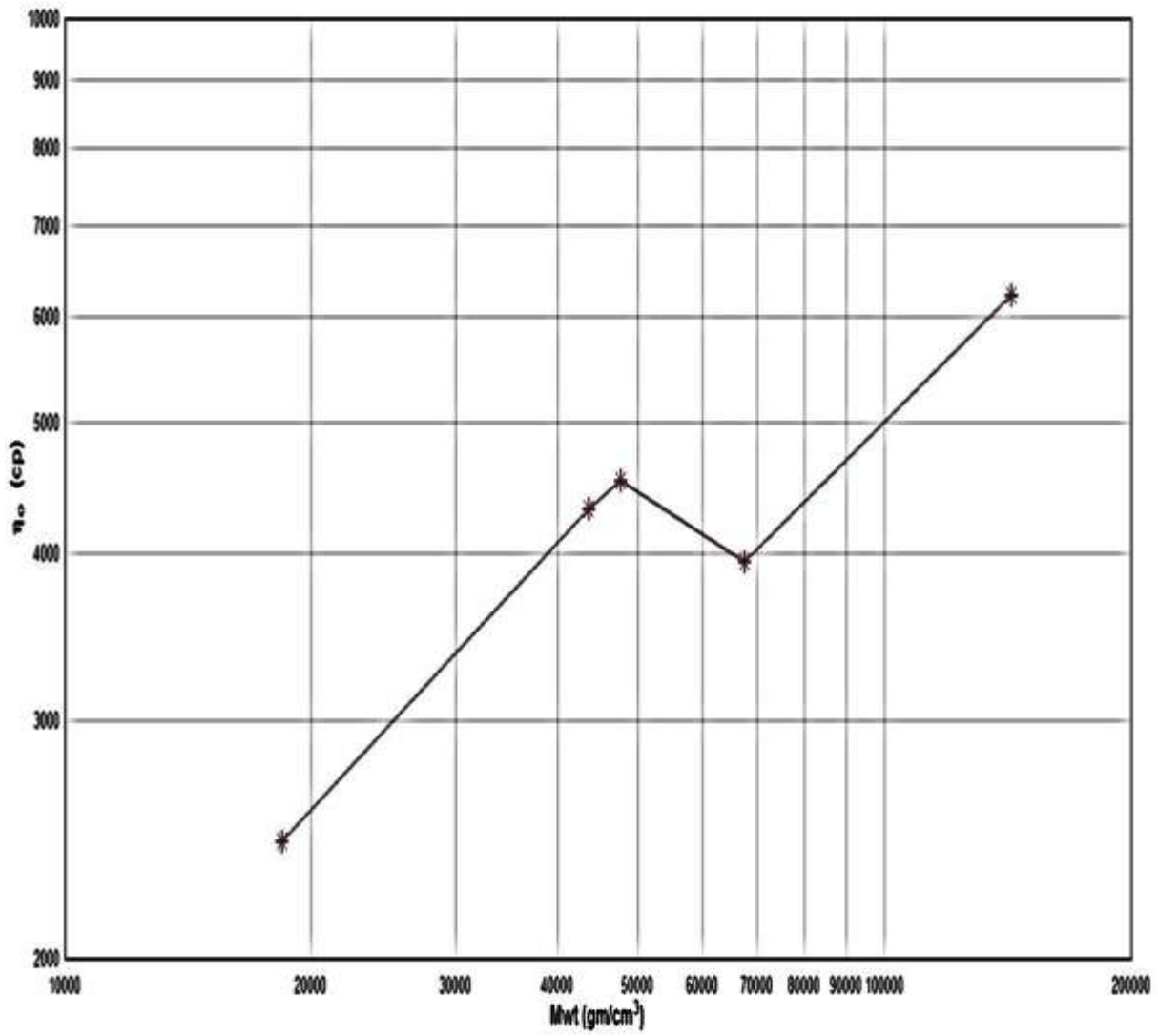


Figure 4.29: Relationship between $\log \eta_0$ and $\log M_v$. for Conc. 4%.

From the figures (4.26 – 4.29) the critical Mwt (M_c) were gotten, and from them the chain element $A(c)$ were calculated from equation (2.27).

$$A(C) = \sqrt[3]{\frac{36}{(\pi \cdot N_L)^2}} \cdot \left(\frac{m_o}{L_o}\right) \cdot \sqrt[3]{\frac{1}{M_e \cdot C^2}} \quad \dots (2.27)$$

Table 4-8: M_e and $A(c)$ of CMC for all conc.

C	M_e	$A(c) \text{ \AA}$
0.01	43,582	7.49236E-17
0.02	43,582	1.18934E-16
0.03	75,522	1.29751E-16
0.04	75,522	1.57182E-16

The data in table (4-8) had been plotted in figure (4.30) and by extrapolating $A(C)$ to zero concentration, to obtained the true chain element $A(0)$

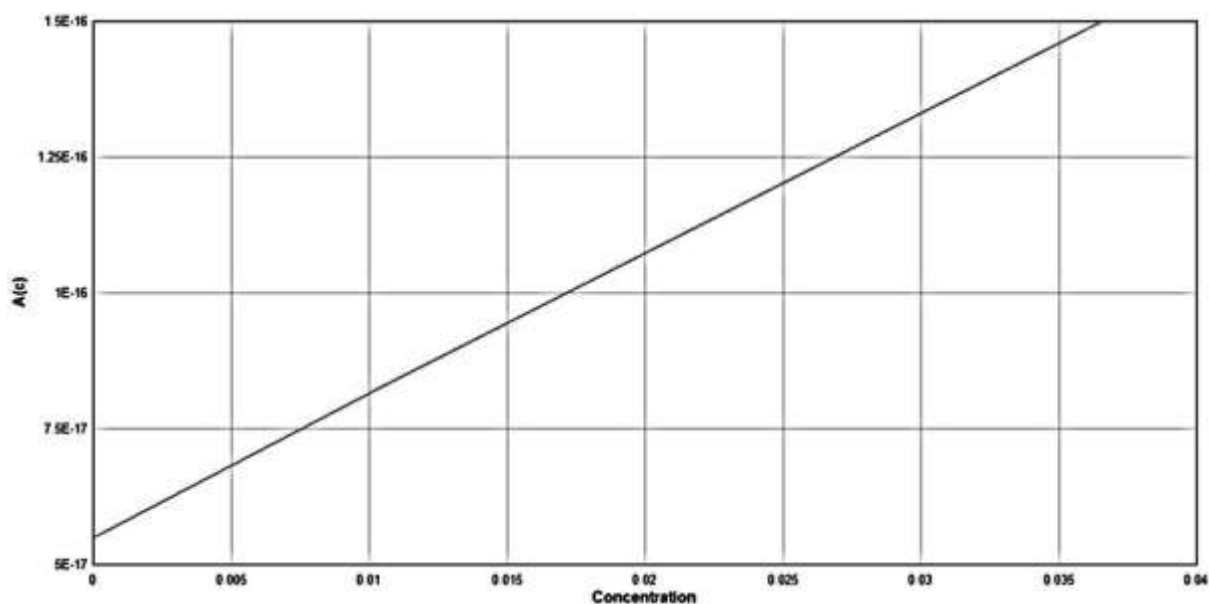


Figure 4.30: Relationship between $A(c)$ and Conc.

the true chain element $A(0)$ and it's equal $(5.5 \times 10^{-17}) \text{ \AA}$.

The results of rotational viscometer for the viscosity and the RPM (which present indirectly the shear rate) with different Mwt (18,000 – 142,000) gm/cm³ and different concentrations, as shown in tables appendix C.

The plotting of η_o versus Mv in log-log scale in figures (4-28 to 4-31) to determine the critical molecular weight (M_c) from the break point which indicates the transition from particle to network region, and calculating the (M_e) and $A(c)$, then determining the true chain element $A(0)$ and it's equal (5.5×10^{-17}).

These solutions (CMC in 6% NaOH) behave as non-Newtonian liquids (pseudoplastic behavior) which mean that the viscosity decrease with increasing the shear rate and from these curves the viscosity (η_o) have been determined at shear rate = 0.

And then a study have been performed at CMC's solutions at fixed shear rate with variation of time to know that if these solutions have Reopexy or thixotropic characteristics (time dependent fluid) to mean the increasing or decreasing the viscosity with increasing the time, these behaviors not have been seen in these solutions as in figure (4.33)

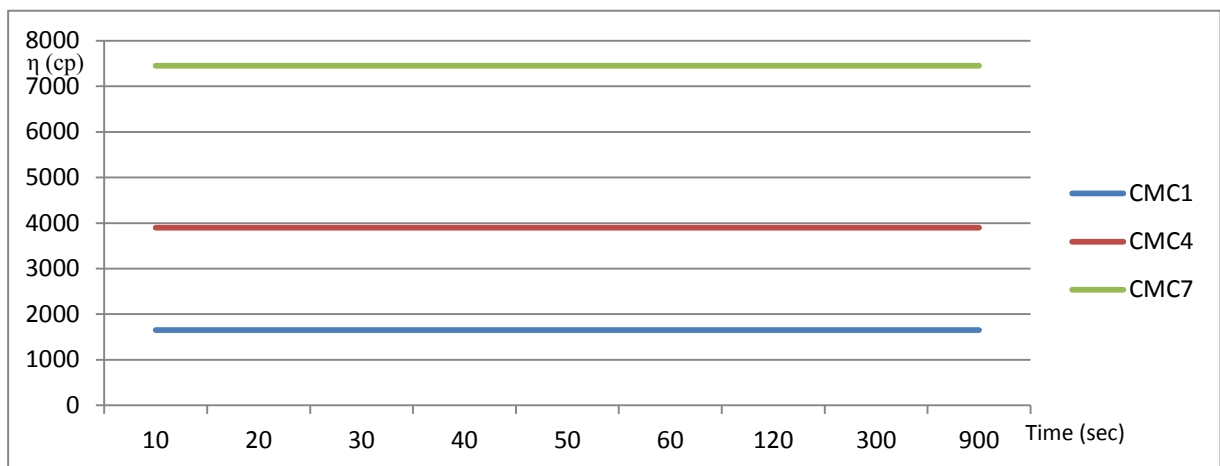


Figure 4.31: Relationship between η and time at fixed RPM (100) for CMC (1,4,7)

CHAPTER FIVE

CONCLUSIONS AND RECOMMENDATIONS

5-1 Conclusions

- 1- The molecular weight of CMC grades which had been used in this work could be estimated through the equation $[\eta] = kMv^a$ and the constant k & a , which are ($k = 7.3 \times 10^{-3}$ and $a = 0.93$) for CMC in (6% NaOH in water).
- 2- Through the measurement of dynamic viscosity for different Mwts and concentrations with plotting (η_o vs Mwt) in log-log scale, the break point found (transition from particle to network M_c) from it the M_e with equation (2.27) to calculate the chain element $A(c)$, and then the true chain element been determined by extrapolating to zero, $A(o) = 5.5 \times 10^{-17}$.
- 3- At fixed shear rate on CMC solutions with variation of time, these solutions showed that they were time independent solutions.

5-2 Recommendations for future work

For those who would carry future studies on the related subject, the following recommendations can be considered:

- 1- Studying the rheological properties for several polymer solutions with high molecular weight to show the effects of large number of atoms present in these molecules.
- 2- Studying the rheological properties of Carboxymethyl cellulose with other solvent or blends of solvents, temperatures, and methods.

REFERENCE

- A. Gabriel, in *Microbial Polysaccharides and Polysaccharases*, Academic Press, 1979, pp. 191–204.
- A. Kondo, T. Irie, and K. Uekama, *Biol. Pharm. Bull.* 19(2), 280–286 (1996). Links
- Al-Dory S.A; *Rheological Study of Polyethylene Glycol Solution*, M. Sc. Thesis, Saddam University, (1999).
- Al-Sa'aidy F.K., *Rheological Study of Phenolic Resin Solution*, M.Sc. Thesis, Saddam University, (1997).
- Anandha Rao M., “*Rheology of Fluid and Semisolid Foods Principles and Applications*”, New York, 1999.
- Aroon V. Shenoy, “*Rheology of Filled Polymer Systems*”, Netherlands, 1999.
- August, *Reference Document on Best Available Techniques in the Production of Polymers*, European Commission, 2007.
- Barnes H.A., Hutton J.E, and Walters K. F. R. S. “*An Introduction to Rheology*”, London, 1989.
- Bernhardt E. C. and Kelvey J. M., “*Polymer Processing – New Engineering Specialty*”, Vol. 35, (July) 154–155, (1958).
- Bocek, Yusupova, and Petropavlovskii, *Russian Journal of Applied Chemistry*, vol. 75, no 4, 2002, pp. 645-648. Translated from *Zhurnal Prikladnoi Khimii*, vol. 75. No. 4, 2002, pp. 659 663.
- Bodanecky M. and Kovar J., *Viscosity of Polymer Solutions*, Elsevier, Amsterdam, 1982.

- Brant D. A. and Buliga G. S., in R. R. Colwell, ed., *Biotechnology of Marine Polysaccharides*, Hemisphere Publishers, Washington, D.C., pp. 30–73, 1985.
- Breene B. I., Orenstein J., and Schmitt-Rink S., *Science*, Vol. 247, 679, 1990.
- Buche F., *Physical Properties of Polymers*; Interscience, New York, (1962).
- Business Communications Company, July, 1994, 00039104.
- Business Communications Company, July, 1994, 00039109.
- Business Communications Company, November, 1996, 00065453.
- Cormick Mc. L., “Water-Soluble Polymers”, *Encyclopedia of Polymer Science and Technology*, Vol. 12, P. 452, 2005.
- D.G. Kessel, Status Report, German Institute for Petroleum Research, 1988, p. 41.
- D.S. Roy and B.D. Rohera, *Pharm. Res.* 13(9), 320 (1996).
- E.I. Sandvik and J.M. Maerker, in *ACS Symp. Series No. 45, Extracellular Microbial Polysaccharides*, 1977, pp. 242–264.
- Eich M., Reck B., Yoon D.Y., Wilson C.G., and Bjorklund G. C., *J. Appl. Phys.*, Vol. 66, 3241, 1989.
- Elliott A. and Ambrose E. J., *Discuss. Faraday Soc.*, Vol. 9, 246 1950.
- Eur. Pat. 611824 (1994), French Institute for Petroleum.
- *Food Chemical News* 12 Feb. 37(51), 15 (1996).
- Fred J. Davis, “*Polymer Chemistry*”, New York, 2004.
- Fredrickson A. G., “*Principle and Application of Rheology*”, Prentice Hall, 1964.

- G. Holzward and E.B. Prestridge, *Science* 197, 757–759 (1977). [Links](#)
- G. Holzward, *Carbohydr. Res.* 66, 173 (1978).
- G. Muller, M. Anrhourrache, J. Lecourtier, and G. Chauveteau, *Int. J. Biol. Macromol.* 8, 167–172 (1986). [Links](#)
- Garito A. F., presented at Pacificchem '89, Honolulu, Hawaii, December 1989.
- Gebhard Schramm, “A Practical Approach to Rheology and Rheometry”, 2nd edition, Germany, 2000.
- GertStrobl, “The Physics of Polymers”, 3^{ed} edition, New York, 2007.
- Gowariker V. R., Viswanathan N. V., and Sreedhav J., “Polymer Science”, Indea, 1987.
- Gruber E., Lederer K., Schure J., “Rheometry and Structure Rheology of Biopolymers”, New York, 1988.
- H. Kumagai, C.H. Chu, T. Sakiyama, S. Ikeda, and K. Nakamura, *Biosci. Biotechnol. Biochem.* 60, 1623–1626 (1996). [Links](#)
- H. McIntyre, H.J. Ceri, and Vogel, *Starch. Starke* 48 (7–8), 285–291 (1996).
- Hadjichristidis, N.; Iatrou, H.; Pispas, S.; Pitsikalis, M. J., *Poly. Sci., Part A: Polymer. Chem.*, Vol. 38(18), 3211–3234, 2000.
- Happy Household & Personal Products Industry, *April*, 33(4), 136 (1996).
- J. Klein and A. Schumpe, *Chem. Ing. Tech.* 66(2), 234–238 (1994).
- J. Sujjaareevath, D.L. Munday, P.J. Cox, and K.A. Khan, *Int. J. Pharm.* 139(1–2), 53–62 (1997). [Links](#)
- J.D. Ntawukulliyayo, S.C. DeSemedt, J. Demeester, and J.P. Remon, *Int. J. Pharm.* 128(1–2), 73–79 (1996). [Links](#)

- James E. Mark, “Physical Properties of Polymers Handbook”, 2nd edition, New York, 2007.
- Jan W. Gooch, “Encyclopedic Dictionary of Polymers”, United States of America, 2007.
- Johannes Karl Fink, “Reactive Polymers Fundamentals And Applications”, United States of America, 2005.
- K. Shimada, H. Okada, K. Matsuo, and S. Yoshioka, *Biosci. Biotechnol. Biochem.* 60, 125–127 (1996). [Links](#)
- K.P. Shatwell, I.W. Sutherland, and S.B. Ross-Murphy, *Int. J. Biol. Macromol.* 12, 71–78 (1990). [Links](#)
- K.P. Shatwell, I.W. Sutherland, S.B. Ross-Murphy, and I.C.M. Dea, *Carbohydr. Polymers* 14, 115–130 (1991).
- K.P. Shatwell, I.W. Sutherland, S.B. Ross-Murphy, and I.C.M. Dea, *Carbohydr. Polymers* 14, 131–147 (1991).
- K.S. Kang and D.J. Pettitt, in *Industrial Gums: Polysaccharides and Their Derivatives*, Academic Press, 1993, pp. 341–371.
- Kuhen W., *Journal polymer sci.*, No. 5, p. 519, 1950.
- L.C. Fryer, F.M. Aramouni, and E. Chambers, *J. Food Sci.* 61(1), 245 (1996). [Links](#)
- L.D. Melton, L. Mindt, D.A. Rees, and G.R. Sanderson, *Carbohydr. Res.* 46, 245–257 (1976). [Links](#)
- Levine B. F., Bethea C. G., Thurmond C. D., Lynch R. T., and Bernstein J. L., *J. Appl. Phys.*, Vol. 50, 2523, 1979.

- Lochhead R. Y., in Lochhead R. Y., ed., *Encyclopedia of Polymers and Thickeners for Cosmetics*, Vol. 108, Allured Publishing Corp., pp. 95–135, 1993.
- M. Hassan-Wakkas, Ph.D. Thesis, Technical University of Clausthal, 1995.
- M. Lerner, *Chemical Market Reporter*, June 24, 26, (1996), 12–14 (1996).
- M. Milas, W.F. Reed, and S. Printz, *Int. J. Biol Macromol.* 18, 211–221 (1996). [Links](#)
- Madeline Goodstein, “Plastics and Polymers Science Fair Projects”, United States of America, 2004.
- Mouritz A.P. and Gibson A.G., “Fire Properties of Polymer Composite Materials”, Netherlands, 2006.
- Nevell T. P. and Zeronian S. H., *Cellulose Chemistry and Its Applications*, John Wiley & Sons, Inc., New York, 1985.
- P.E. Jansson, L. Keene and B. Lindberg, *Carbohydr. Res.* 45, 275–282 (1975). [Links](#)
- Pantelis P. and Davies G. J., U.S. Pat., to British Telecommunications, Vol. 4, 748, 1988.
- Pierce R. H., Hickman R.J., Mackenzie E.P., Smith M.J., 5th edition, *Blueprint*, New York, 1993.
- R. Moorhouse, M.D. Walkinshaw, and S. Arnott, *ACS Symp. Ser.* 45, 90–102 (1976).
- R.A. Hassler and D.H. Doherty, *Biotechnol. Prog.* 6, 182–187 (1990). [Links](#)

- Rao D. N., Burzynski R., Mi X., and Prasad P. N., Appl. Phys. Lett., Vol. 48, p. 387, 1986, A.
- Rao D. N., Swiatkiewicz J., Chopra P., Chosal S. K., and Prasad P. N., Appl. Phys. Lett., Vol. 48, p. 1187, 1986, B.
- Salman M. Z., Particle and Network Structure of Polychloroprene Solutions, M.Sc. Thesis, Saddam University, (2000).
- Schiraldi A., Piazza L., Brenna O., and Vittadini E., J. Thermal Analysis, Vol. 47, p. 1339, 1996.
- Schurze J., Journal of Macromolecular Science, No.9, p. 1249, 1996.
- Schurze J., Porg. Polym. Sci., Vol. 16, p. 1, 1991.
- Sperling L.H., “Introduction to Physical Polymer Science”, 4th edition, Canada, 2006.
- Sultan G. A., Rheological Study of Polyvinyl Alcohol Solution, M.Sc. Thesis, Saddam University, (1998).
- The Royal Society of Chemistry, Press release, Oct. 23, 1996.
- Tveskov V. N., Eskin V. y., Frenkel S. Y., “Structure of Macromolecules in Solution”, London, 1970.
- U. Grove and D. Kessel, Chem. Ing. Tech. 68, 4196, 413–417 (1996).
- U.S. Pat. 3,659,026 (1972), H.R. Schuppner.
- U.S. Pat. 5350528 (1994), Weyerhauser.
- Vlachopoulos J. and Wagner J.R., The SPE Guide on Extrusion Technology and Troubleshooting, Society of Plastics Engineers, Brookfield, 2001.
- Zehev Tadmor and Costas G. Gogos, “Principles of Polymer Processing”, 2nd edition, Canada, 2006.

Appendix A

Table A-1: Values of the Mark–Houwink–Sakurada exponent a [Sperling, 2006].

a	Interpretation
0	Spheres
0.5–0.8	Random coils
1.0	Stiff coils
2.0	Rods

Appendix B

Table B-1: The results of CMC1 measurements with capillary viscometer.

Concentration (gm/cm³)	Flow Time (s)	η_{sp}(cp)	η_{red}(cp)
0.001	16.70	0.072575466	72.57546564
0.002	18.00	0.156069364	78.03468208
0.003	19.45	0.249197174	83.06572468
0.00334	19.98	0.283236994	84.80149528
0.005	22.84	0.466923571	93.38471419

Table B-2: The results of CMC2 measurements with capillary viscometer.

Concentration (gm/cm³)	Flow Time (s)	η_{sp}(cp)	η_{red}(cp)
0.001	18.02	0.157353886	157.3538857
0.002	20.68	0.328195247	164.0976236
0.003	23.56	0.513166346	171.0554485
0.00334	24.59	0.579319204	173.4488634
0.005	29.94	0.922928709	184.5857418

Table B-3: The results of CMC3 measurements with capillary viscometer.

Concentration (gm/cm³)	Flow Time (s)	η_{sp}(cp)	η_{red}(cp)
0.001	19.54	0.254977521	254.9775209
0.002	26.46	0.699421965	349.7109827
0.003	36.13	1.320488118	440.1627061
0.00334	40.03	1.570969814	470.3502436
0.005	64.23	3.125240848	625.0481696

Table B-4: The results of CMC4 measurements with capillary viscometer.

Concentration (gm/cm³)	Flow Time (s)	η_{sp}(cp)	η_{red}(cp)
0.002	24.12	0.549132948	274.566474
0.0025	26.72	0.716120745	286.448298
0.00334	31.51	1.023763648	306.5160623
0.005	42.60	1.736030829	347.2061657

Table B-5: The results of CMC5 measurements with capillary viscometer.

Concentration (gm/cm³)	Flow Time (s)	η_{sp}(cp)	η_{red}(cp)
0.0015	26.59	0.707771355	471.8475701
0.001667	27.87	0.789980732	473.8936606
0.002	30.45	0.955684008	477.8420039
0.0025	34.41	1.210019268	484.0077071
0.00334	41.28	1.651252408	494.3869486
0.005	55.61	2.571612075	514.3224149

Appendix C

Table C-1: η and RPM of each CMC sample with Conc. 1%.

CMC sample no.	η(cp)	RPM
CMC1	81.4	60
	79	100
	76	200
CMC2	89	30
	75	50
	69	60
	55	100
	46	200
CMC3	148	30
	143	50
	141	60
	137	100
CMC4	135	60
	110	100
	77	200
CMC5	210	20
	200	30
	181	50
	172	60
	150	100

Table C-2: η and RPM of each CMC sample with Conc. 2%.

CMC sample no.	η(cp)	RPM
CMC1	580	60
	520	100
	430	200
CMC2	670	30
	510	50
	476	60
	389	100
	300	200
CMC3	1001	30
	920	50
	900	60
	820	100
CMC4	950	60
	790	100
	570	200
CMC5	1600	20
	1459	30
	1230	50
	1150	60
	900	100

Table C-3: η and RPM of each CMC sample with Conc. 3%

CMC sample no.	η(cp)	RPM
CMC1	674	50
	650	60
	610	100
	580	200
CMC2	1225	50
	1210	60
	1175	100
	1130	200
CMC3	1460	20
	1380	30
	1310	50
	1300	60
	1270	100
CMC4	1500	30
	1350	50
	1300	60
	1260	100
CMC5	2600	20
	2510	30
	2412	50
	2377	60
	2258	100

Table C-4: η and RPM of each CMC sample with Conc. 4%.

CMC sample no.	η(cp)	RPM
CMC1	2340	50
	2200	60
	1950	100
	1650	200
CMC2	4002	50
	3920	60
	3780	100
	3600	200
CMC3	4550	20
	4250	30
	3900	50
	3750	60
	3350	100
CMC4	4400	30
	3900	50
	3700	60
	3095	100
CMC5	6000	20
	5680	30
	5200	50
	5000	60
	4500	100
	7450	100

الْخُلَاصَة

اجريت دراسة ريولوجية على محاليل carboxymethyl cellulose (CMC) حيث تم اذابة المادة في محلول (٦% هيدروكسيد الصوديوم في الماء)، واستخدمت سبعة اوزان جزيئية مختلفة من بوليمر (CMC) carboxymethyl cellulose.

لغرض تحديد الاوزان الجزيئية تم قياس اللزوجة في المزلاج الشعري والحصول على قيم intrinsic viscosity (staudinger index or)، ومنها تقدير الوزن الجزيئي لهذه الاوزان من خلال معادلة (Mark – Houwink) : $[\eta] = kMv^a$ ، وقد تم الحصول على قيم K_H Huggins (coefficient) من رسوم (η_{red} vs conc.).

كما تم قياس منحنى الجريان للاوزان الجزيئية المختلفة وبتراكيز مختلفة ومن ثم تم تحديد اللزوجة (η_0) عند معامل قص صفر، عند رسم ($\log \eta_0$ vs $\log Mwt$) والذي منه قد نستطيع تحديد الوزن الجزيئي الحرج (M_c) والذي يمثل نقطة التحول من particle الى network region.

شكر وتقدير

بعد شكر الله عز وجل اود أن أتقدم بأسمى آيات الشكر والتقدير للدكتور طالب كشمولة مشرفاً" لما بذله من مجهود لأعطاء هذا النتاج العلمي.

كما اتقدم بالشكر والتقدير الى رئيس قسم الهندسة الكيمياوية لتعاونه ودعمه لهذا المشروع العلمي كما اتقدم بالشكر الى عمادة كلية الهندسة لما قدمته من تعاون لاكمال رسالتي.

كما لاننسى ان نتقدم بالشكر والامتنان الى شركة الزيوت النباتية وبالاخص قسم (البحث والتطوير - مختبر البحوث والبداثل) وقسم (ضبط الجودة - مختبر المواد الاولية) لابدائهم المساعدة اللازمة لاجراء جميع الفحوصات اثناء فترة البحث.

أتقدم بالشكر و التقدير الكبيرين الى من كانا الدافع وراء حصولي على شهادة الماجستير امي وابي.

الى من كانوا معي خطوة" بخطوة اخي واختي.

من رافقوا دربي اصدقائي.

دراسة ريولوجية تركيبية لمحاليل

كاربوكسي مثل سليولوز

رسالة

مقدمه إلى كلية الهندسه في جامعة النهريين

وهي جزء من متطلبات نيل درجة ماجستير علوم

في الهندسه الكيمياويه

من قبل

مصطفى جعفر نايف

(بكالوريوس علوم في الهندسة الكيمياوية ٢٠٠٦)

١٤٣٢

صفر

٢٠١١

شباط